Eye-Movement-Controlled Wheelchair Based on EOG for People with Quadriplegia

Project team:

Anas shaer **Yazan nazzal**

Supervisors:

Eng. Ali Amro

Submitted to the College of Engineering in partial fulfillment of the requirements for the degree of Bachelor degree in Biomedical Engineering

Hebron , 2022

الإهداء

إلى معلمنا و قائدنا و قدوتنا وشفيعنا سيدنا محمد عليه أفضل الصلاة و أتمّ التسليم

إلى من اصطفاهم الله ليرسموا طريق الحرية بدمائهم, شهداءنا الأبرار

إلى من ضحّوا بأعمارهم خلف قضبان سجون الإحتلال , أسرانا البواسل

إلى من سطّروا بأمعائهم الخاوية أروع ملاحم الفخر و البطولة, الأسرى المضربين عن الطعام

إلى قبلتنا الأولى, إلى رمز كرامتنا و عزّنا, إلى الذي أقصى غاياتنا أن نصلي فيه ولو ركعة رباط, لكل حجر إسلامي عربي في المسجد الأقصى

الى اللواتي رأيننا بقلبهن قبل أعينهن, الى من هي الجنة تحت أقدامهن, إلى أمهاتنا العزيزات

إلى من يصلون النهار بالليل من أجلنا, إلى آبائنا الكرام

إلى من نفتخر بهم, إلى سندنا أخوتنا و أخواتنا الأحبّاء

إلى من حفروا في قلوبنا قبل عقولنا منارات الأخلاق و العلم, إلى من سيبقى فضلهم –من بعد الله- تاجاً على رؤوسنا, معلمينا و معلماتنا الأكارم

إلى من شقّ معنا طريق النجاح, إلى من نفتخر ونعتز بإشرافه علينا, الأستاذ علي عمرو

إلى من لم يبخلوا بأي شيء لدعم مشروعنا, جمعية الرحمة و الشيخ صالح عقل

إلى مصدر فخرنا وعزنا, إلى صرحنا العظيم, جامعة بوليتكنك فلسطين

Abstract

The number of disabled people is increasing at a rapid rate, disability to control limbs due to accidents and wars are the major cause of immobility. Immobility hinders daily activities and leads to social restrictions which isolate them from the rest.

Forfeiture of the ability of quadriplegic people to control their hands isa serious challenge in designing wheelchairs that meet their needs. The aim of this project is to invest the eyes and tongue movements of quadriplegic people to design a motorized wheel chair controlling system capable of receiving the digital output from an electrooculographic amplifier and filter, to analyze these electrooculograms (EOGs) electronically for controlling wheel chair movements, and pressure sensor, to enable these people control the activation and deactivation of the eye-controlling-system.

For more accuracy, the flexiForce sensor mounted on the cheek recipes pushes from the tongue, it is used to ON/OFF eye-controlling-system, which helps the patient to look freely when he/she don't need it and just want to walk straight .

الملخص

عدد المصابين بالإعاقات الحركية بإرتفاع متزايد, فقدان القدرة على التحكم بالأطراف بسبب الحوادث و الحروب هو سبب رئيسي للإعاقات الحركية, الإعاقات الحركية تحد من القدرة على إتمام الأنشطة اليومية و الاجتماعية للمصاب مما يساهم بعزله عن المجتمع. أيضا, فقدان القدرة على التحكم بالأيدي للمصابين بالشلل الرباعي هو تحدٍ صعب يعقد عملية تصميم كرسي متحرك يلبي احتياجاتهم.

فقدان القدرة على التحكم بالأيدي عند المصابين بالشلل الرباعي يشكل تحدِ جدّي في بناء كرسي متحرك يلبي إحتياجاتهم . الهدف من هذا المشروع هو استثمار حركات العين و اللسان للمصابين في تصميم نظام تحكم للكرسي الكهربائي قادر على استقبال الناتج من عملية تكبير و ترشيح الإشارة الكهربائية للعين لتحليل هذه الإشارة للتحكم بحركة الكرسي, مع حساس ضغط حتى يستطيع المستخدم تشغيل و إيقاف تشغيل نظام القيادة بالعين.

للزيادة في الأمان, تم إضافة حساس مُثبت على الخد يستقبل الضغطات من اللسان, بحيث يستطيع المريض أن يستخدمه لتشغيل و إيقاف تشغيل نظام القيادة بالعين, مما يجعل المريض يستطيع النظر بشكل حر عندما لا يريد تشغيل نظام القيادة بالعين , و يريد فقط أن يسير بشكل مستقيم.

Contents

CHAPTER THREE

THEORETICAL BACKGROUND

CHAPTER FOUR

SYSTEM DESIGN

CHAPTER FIVE

TESTING AND RESULTS

List of Table

List of Figures

Table of Abbreviations

Abbreviation	Full Word
EOG	Electrooculography
Hz	Hirtz
mV	Millivolts
mA	Milliampere
V	Volts
dB	Decibel

Chapter one

Introduction

1.2 PROJECT IDEA

1.3 LITERATURE REVIEW

1.4 PROJECT MOTIVATION

1.5 PROJECT OBJECTIVES

1.6 PROJECT IMPORTANCE

1.7 PLAN OF WORK

1.8 TIME LINE

1.9 Budget

1.1 Introduction:

Quadriplegia, also known as tetraplegia, is a form of paralysis that affects all four limbs,plus the torso ("quad" originates from the Latin word for four). Most people with tetraplegia have significant paralysis below the neck, and many are completely unable to move.[1]

The basic symptoms of quadriplegia include numbness/loss of feeling in the body, particularly in the arms and legs, paralysis of the arms and legs (and major muscles in the torso), urinary retention and bowel dysfunction caused by lack of muscle control, difficulty breathing (some quadriplegics require assisted breathing devices), and trouble sitting upright (because of an inability to balance).

Controlling wheelchairs by eyes movements is a leading technology in improving the quality of the life for paralyzed peoples, specially who are suffering from Quadriplegia. EOG, Infrared, magnetic scleral search coil and video-based eye tracking are used methods to achieve this technology.

1.2 Project Idea:

The idea of this project is to provide the people with quadriplegia with automated wheelchair that has the ability to move according to their eye movements by acquiring their EOG signals and processing them to control the wheelchair direction according to the table 1.1.

Table1.1: Control Eye Movements

Control Eye Movements	Wheelchair Directions
Gaze to the right	Turn to the right
Gaze to the left	Turn to the left
Upward gazing	OFF DC motors

A pressure sensor will be mounted on the cheek to differentiate between control eye movements and normal eye movements, in which one press will ON/OFF the eye-drive-system, which consists of gazing right and left, where upward gazing is activated alone all the time, to let the user to control the DC motors any time he/she want

1.3 Literature Review

This project comes to accomplish the previous project and studies in the fields of analyzing EOG and controlling wheelchairs using eye movements.

Several methods are used in eye tracking as infra-red technology, video oculography with

camera system, EOG and some other old methods like sceleral search coils in order to control wheelchairs using eye movements, It was obvious that EOG tracking is a lower cost and less complicated system. [2]

Low cost, user friendly, and high efficient eye controlled wheelchair will be the best choice for quadriplegic people for more life quality.

1.4 Project motivation:

75 million people are in need of a wheelchair but cannot afford one!

According to a survey published in 2019 by the National Spinal Cord Injury Statistical Center (NSCISC), which is a spinal cord injuries statistical center in USA, the top causes of spinal Cord Injuries are divided as shown in figure 1.1.

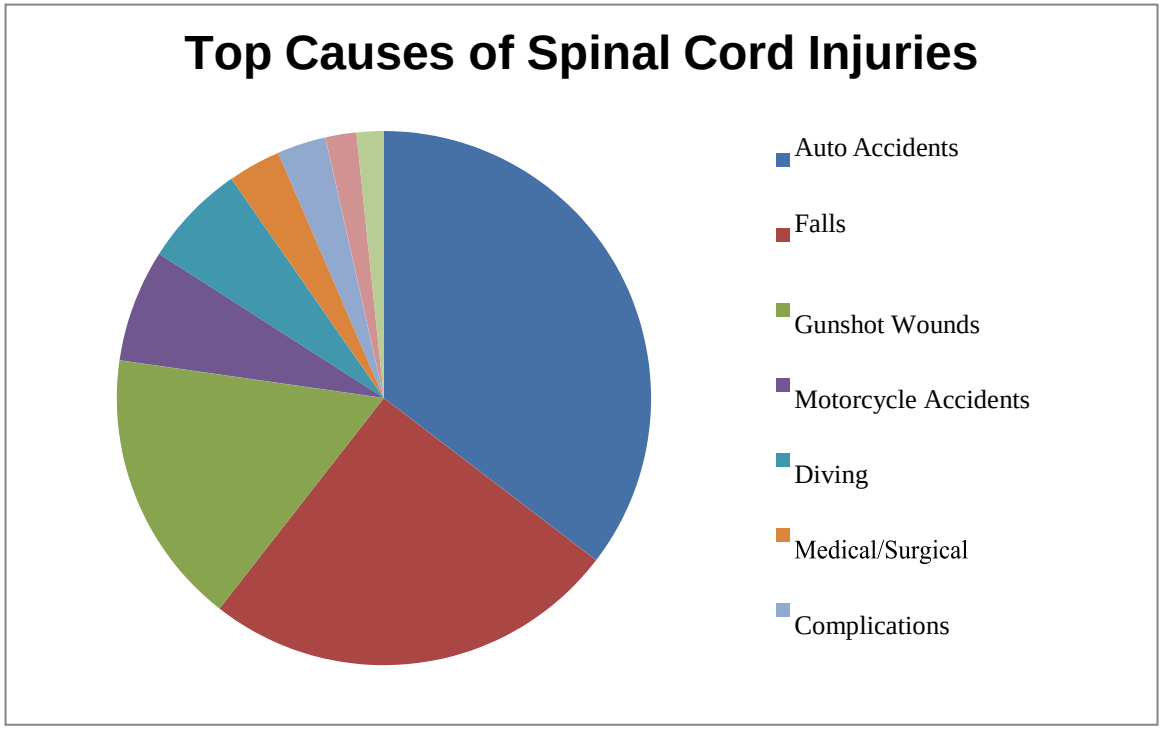

Figure 1.1: Top Causes of Spinal Cord Injuries by NSCISC

In the chart above we can see that there are many common causes; as auto accidents and gunshot wounds, this shows the importance of sharing the improving wheelchair controlling technology, especially to fit the needs of people with quadriplegia.

The zionist occupation is a regional example of the gunshots cause of quadriplegia, there is an increasing number of injured people with paralysis concentrated in Gaza strip and West bank. [3]

As well, according to the Palestinian Central Bureau of Statics (PCBS), there is a prominent number of car accidents in Palestine, those accidents will increase the number of

paralyzing injures[4]. Also, according to PCBS, the mobility injures have the highest ratios in both the west bank and Gaza strip as shown in the figure 1.2. [5]

نسبة ذوي الاعاقة في فلسطين* حسب نوع الإعاقة، المنطقة والجنس، 2017
Percentage of Disabled in Palestine* by Type of Disability, Region and Sex, 2017

Type of Disability	Region						المنطقة			نوع الإعاقة
	قطاع غزة Gaza Strip			الضفة الغربية West Bank			فلسطين Palestine			
	إناث Females	ذكور Males	المجموع Total	إناث Females	ذكور Males	المجموع Total	إناث Females	ذكور Males	المجموع Total	
Seeing	0.7	0.9	0.8	0.5	0.6	0.6	**0.6**	**0.7**	**0.7**	البصر
Hearing	0.5	0.6	0.5	0.4	0.4	0.4	**0.4**	**0.5**	**0.5**	السمع
Communication	0.5	0.6	0.5	0.4	0.4	0.4	**0.4**	**0.5**	**0.4**	التواصل
Mobility	1.3	1.4	1.3	0.8	0.9	0.9	**1.0**	**1.1**	**1.1**	الحركة واستخدام الأيدي
Remembering and Concentration	0.5	0.5	0.5	0.3	0.4	0.4	**0.4**	**0.4**	**0.4**	التذكر والتركيز

Note: Disability includes a lot of difficulty, and can't at all. ملاحظة: الاعاقة تشمل صعوبة كبيرة، ولا يستطيع مطلقا.

* Data exclude those parts of Jerusalem governorate which were annexed by Israeli Occupation in 1967. * البيانات لا تشمل ذلك الجزء من محافظة القدس والذي ضمه الاحتلال الإسرائيلي إليه عنوة بعيد احتلاله للضفة الغربية عام 1967

Figure 1.2: Mobility Injuries Ratios According to PCBS

Although of the number of paralyzed people in Palestine, there are no wheelchairs that meet the needs of full paralyzed people, even if requested; its cost will be very high.

The EOG-based controlling method -compared to other methods- is a low cost in controlling wheelchairs.

1.5 Project objectives:

1- Design an EOG system to acquire the control eye movements.

2- Control the motors (DC and Servo) according to the control eyes movements.

3- Achieve a safe, effective, and low-cost wheelchair which will empower full-paralyzed persons to control their wheelchairs by eye movements.

1.6 Project importance:

1- Low-cost of the EOG system

2- Lack of eye-controlled wheelchairs in Palestine

1.7 Plan of work:

First, we will implement the electronic system which will acquire, filter, and amplify the EOG signal from the eye, then, we will build the algorithm which will analyze and classify the processed EOG signal and control the motors.

1.8 Time line:

Time schedule of the work for the first semester and second semesters are shown in tables 1.3 and 1.4.

Table 1.3: Time Line for the First Semester

Week / Activities	1	2	3	4	5	6	7	8	9	10	11	12	13	14	15
Finding Project Idea															
Proposal															
Search and Collecting Data															
Documentation															
Preparing for Presentation															
Print Documentation															

Table 1.4: Time Line for the Second Semester

Week / Activities	1	2	3	4	5	6	7	8	9	10	11	12	13	14	15
Implementation															
Testing															
Documentation															

1.9 Budget:

Cost in dollar is distributed as shown in the following table:

Table 1.5: Project Cost

Component		Quantity	Price for each component	Price $
Electrodes wires		5	4	20
Electrodes paddles		20	3	60
FSR406 FelxiForce sensor		1	25	25
Switch button	20A switch button	5	4	22
	4A switch button	1	2	
Motor Driver		1	73	73
PCB Boards			9	9
IC's:	AD620	2	10	19
	AD822	2	9	
Resistors & Capacitors		26	-	3.5
Connection Wires	1mm wire	10 meter	-	13.5
	5 mm wires	5 meter	-	
	2mm wire	5 meter	-	
	3×3mm wire	6 meter	-	
Sockets		20	-	1
Plastic cleats		2	3	6
Battery		2	15	30
Wheelchair battery		2	350	700
Wheelchair battery Charger		1	100	100
Puma 40 wheelchair		1	7000	7000
Total Price		-	-	**8082 $**

Chapter Two

The Anatomy of Human Eye and Spinal Cord.

2.1 Introduction:

Two vital components of the human body; eye and spinal cord, the spinal cord is divided into four parts: cervical, thoracic, lumbar, and sacral spines, each contains several vertebras which have an array of nerve cells (grey matter) and axons (white matter) sending the brain messages to the body. The human eye consists mainly of the cornea and retina which creates the potential difference to make the eye movements which is the EOG signal.

In this chapter, we will discuss the anatomy of the eye and spinal cord, and we will know more about spinal cord injuries especially the quadriplegia and its degrees which will be so important to know the exact health circumstances of the target patients to provide the best health care.

2.2 Foundation of EOG

In this section, we will outline the human eye anatomy to be familiar with how the EOG will be created.

Figure 2.1 shows the basic components of the eye when there is an active nerve in the retina, an increasing potential with right gaze, and a decreasing potential of left gaze between it and the cornea will be founded, figure 2.2 shows the EOG signal for horizontal and vertical eye movements, this potential difference is the EOG signal which can be used as an indication to know the activity of the eye like gaze direction and blinking by detecting it using surface electrodes mounted as shown in figure 2.3.

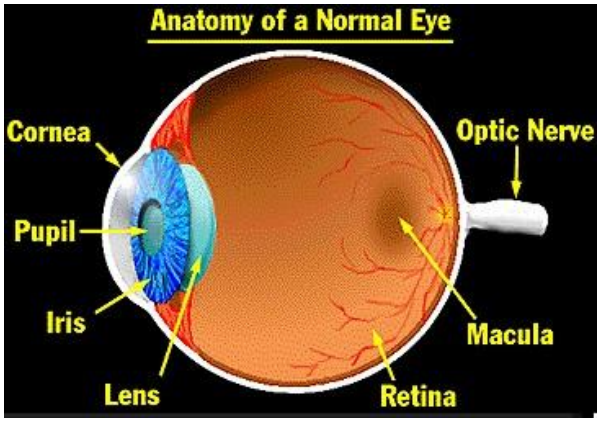

Figure2.1: The Anatomy of The Eye

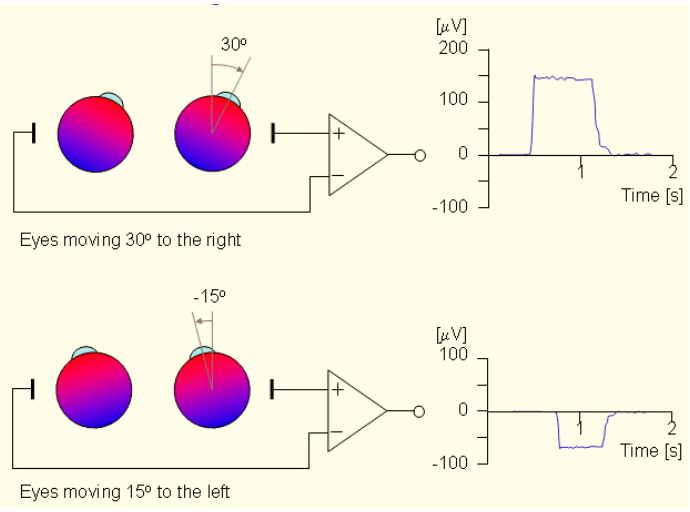

Figure 2.2(a): Right and Left EOG Signal

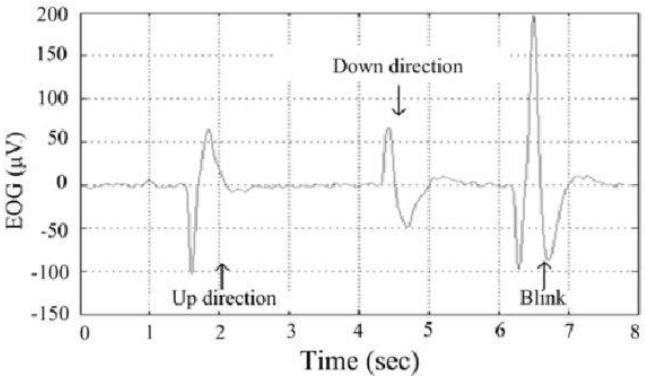

Figure 2.2(b): Vertical and Blink EOG[1]

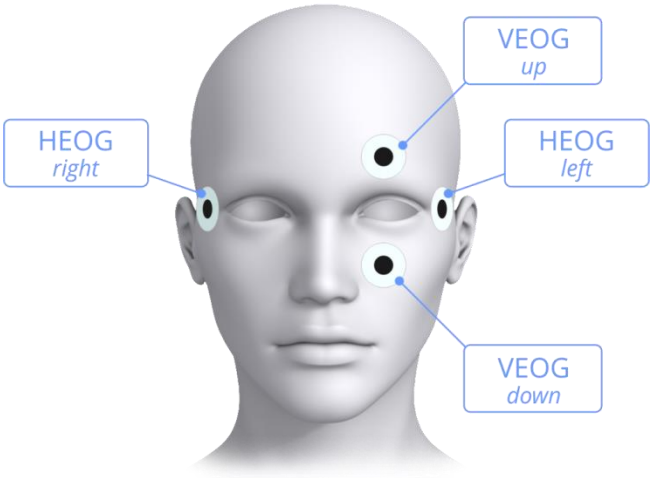

Figure 2.3: The Placement of the EOG Electrodes.

2.2.1 Physiological Background

The eye movements are controlled by three separate pairs of muscles, including the medial and lateral recti and the superior and inferior recti and oblique as shown in figure 2.3.

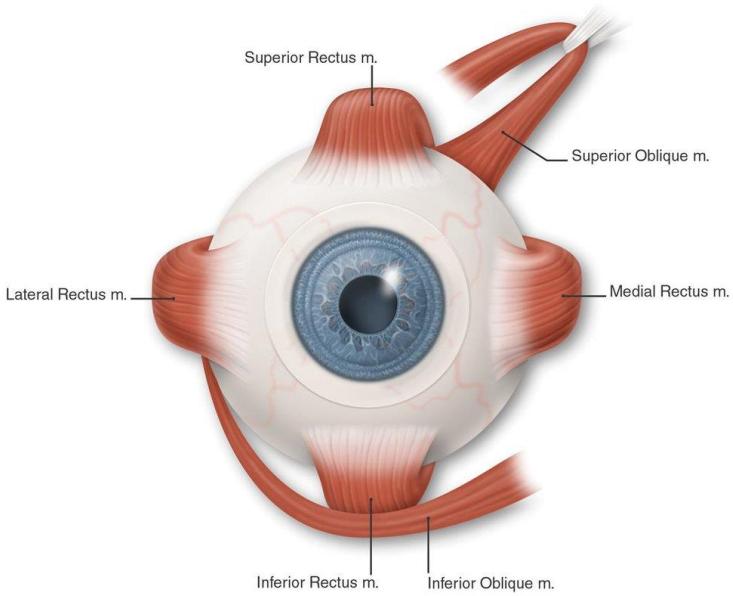

Figure 2.4: eye muscles

The function of these muscles is to stabilize and move the eye in a different directions, the distribution of the muscles is symmetrical. Each of the three sets of muscles to each eye is reciprocally innervated so that one muscle of the pair relaxes while the other contracts. Table 2.1 shows the location and action of each muscle.

Table 2.1: Eye muscles location and function

Muscle	Location	Action
Superior rectus	Superior and central part of eyeball	Moves eyeballs superiorly (elevation) and medially (adduction), and rotates them medially.
Inferior rectus	Inferior and central part of eyeballs	Moves eyeballs inferiorly (depression) and medially (adduction), and rotates them medially.
Lateral rectus	Lateral side of eyeballs.	Moves eyeballs laterally (abduction).
Medial rectus	Medial side of eyeballs.	Moves eyeballs medially (adduction).
Superior oblique	Eyeball between superior and lateral recti.	Moves eyeballs inferiorly (depression) and laterally (abduction), and rotates them medially
Inferior oblique	Eyeballs between inferior and lateral recti.	Moves eyeballs superiorly (elevation) and laterally (abduction) and rotates them laterally

2.3 Spinal Cord

The spinal cord is a bundle of nerve fibers and tissue which lies within spine forming the brain's connection to the body, any malfunction of it will cause a serious injury will affect the sensation and movements of the body limbs and organs, one of the dangerous spinal cord injuries is paralysis with all of its types, the one we will deal with is the quadriplegia.

2.3.1 Spinal Cord Anatomy and injuries

The spinal cord is encased within ring-shaped bones called vertebrae. Both the spinal cord and the corresponding vertebrae are covered with a protective membrane which together forms the spinal column (or backbone), figure 2.5 shows the vertebras of the spinal cord.

A spinal cord injury is the result of damage to any portion of the spinal cord or the nerves at the base of the spine. Damage to any part of the spinal cord can impact sensory, motor, and reflex capabilities because the brain is unable to send information to the body.

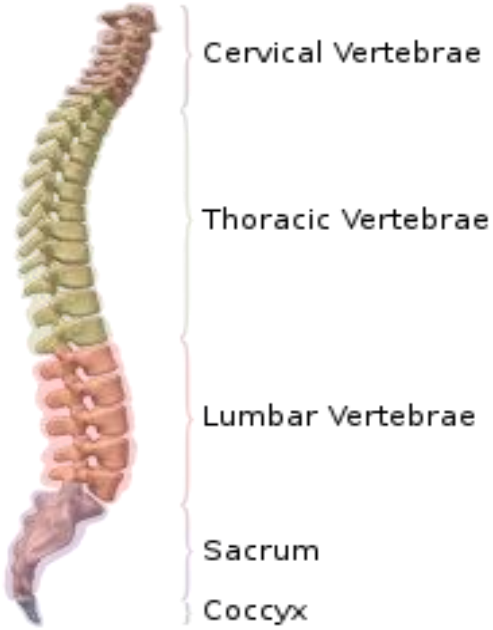

Figure 2.5: The Vertebras of the Spinal Cord

The spinal cord itself contains an array of nerve cell bodies (grey matter) and axons (white matter) running from the brain to the body with peripheral nerves exiting at openings throughout the vertebrae,

The central nervous system contains more than 100 billion neurons. Neurons are the simplest units that make up the nervous system and are similar to the makeup of any other cell within the body except for their vast potential to relay information through chemical and electrical signals, there are four types of neurons:

1. **Motor neurons**: Neurons that relay messages between muscles, organs, and glands.
2. **Sensory neurons:** Neurons that send signals to the brain and spinal cord from external stimuli and internal organs.
3. **Interneurons**: Neurons that relay signals between sensory and motor neurons.
4. **Receptors:** Neurons that collect information from the environment and communicate messages through the sensory neurons.

The spinal cord is divided into four sections, each controls a part of the body as shown in figure 2.7:

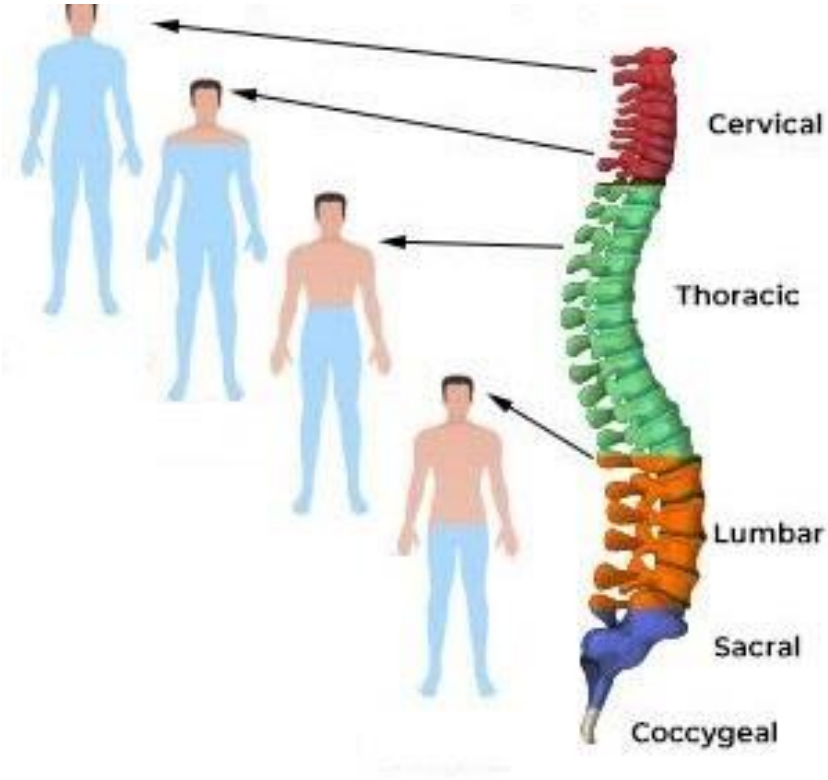

Figure 2.7: Spinal Cord Parts and its Associated Body Parts.

2.3.1.1 Cervical spine

The cervical spine is located at the very top of the spinal column as shown in figure 2.7. The seven vertebral levels within this region, which are classified as C1-C7 from the top-down, form the human neck.

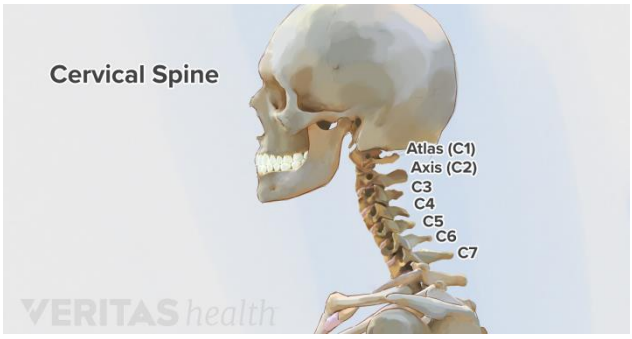

Figure2.7: The Cervical Spin

C1, C2: The C1 vertebra, also known as Atlas, along with the C2 vertebra, also known as Axis, are the first two segments in the cervical spine. These levels are especially important, as they support the head. The Atlas vertebra pivots on the Axis vertebra which allows the head to rotate.

Injuries to the spinal cord at the C1 & C2 vertebral levels are considered to be the most severe of all spinal cord injuries as they can lead to full paralysis but are most often fatal.

C3, C4, C5: The C3, C4, and C5 vertebrae form the midsection of the cervical spine, near the base of the neck. Injuries to the nerves and tissue relating to the cervical region are the most severe of all spinal cord injuries because the higher up in the spine an injury occurs, the more damage that is caused to the central nervous system.

C6, C7, C8: The C6 and C7 vertebrae are the lowest levels of the cervical spine, near the base of the neck. Injuries to the spinal cord corresponding to these regions of the spine have the potential to impact everything below the top of the ribcage resulting in quadriplegia.

Patients with cervical spinal cord injuries will likely experience to some degree:

- Inability to breathe on one's own without assistance (C1-C4)
- Impaired ability or inability to speak (C1-C4)
- Numbness, tingling, or loss of feeling below the level of the injury
- Paralysis in the legs, torso, and arms
- Inability to control bladder and bowel function
- Inability to groom or dress oneself

2.3.2 Quadriplegia

Quadriplegia refers to paralysis from the neck down, including the trunk, legs and arms. The condition is typically caused by an injury to the spinal cord that contains the nerves that transmit messages of movement and sensation from the brain to parts of the body.

C5,C6, and C7 vertebrae are the lowest levels of the cervical spine, near the base of the neck. Injuries to the spinal cord corresponding to these regions of the spine have the potential to impact everything below the top of the ribcage resulting in quadriplegia.

Chapter Three

Theoretical Background

3.1 EOG Amplifier

3.1.1 Surface Electrodes

3.1.2 Pre-Amplifier

3.1.3 Filter

3.2 Pressure Sensor

3.3 Controller

3.4 Motors

3.4.1 DC Motor

3.4.2 Motor Driver

3.4.3 Torque and speed

3.5 Power Switch

3.6 Battery

This chapter provides the theoretical background of the system shown in figure 3.1. Basically, the system mainly consists of EOG amplifier, pressure sensor, controller, and electric motors.

Section 3.1 focuses on the emergence of an electrooculogram (EOG) signals, By the end of this section it should be clear why the EOG signal occur, what they stand for, and what are the EOG amplifier components required to acquire and amplify them to enable the controller read the signals accurately.

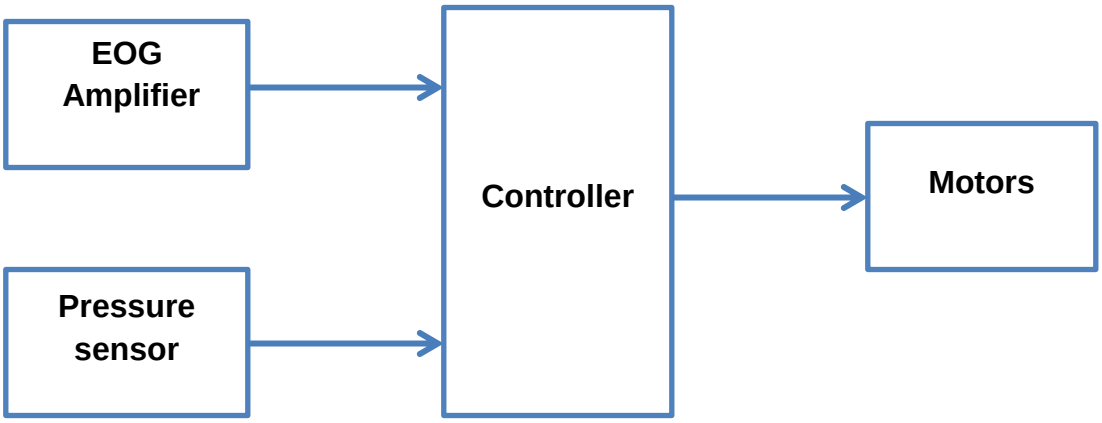

Figure 3.1: General Block Diagram

3.1 EOG Amplifier

An electrooculogram (EOG) is the electric potential measured around the eyes, which is generated by the corneo-retinal standing potential between the front and back of the eye.

EOG signal has been acquired through a two channel system (comprising of a horizontal and a vertical channel) using Ag/AgCl disposable electrodes. The frequency range of EOG signal is 0.1 to 20 Hz and the amplitude lies between 100-3500 micro volts [1]. Pairs of electrodes are generally attached either to the left and right of the eyes (horizontal EOG component), shown in figure 3.2.

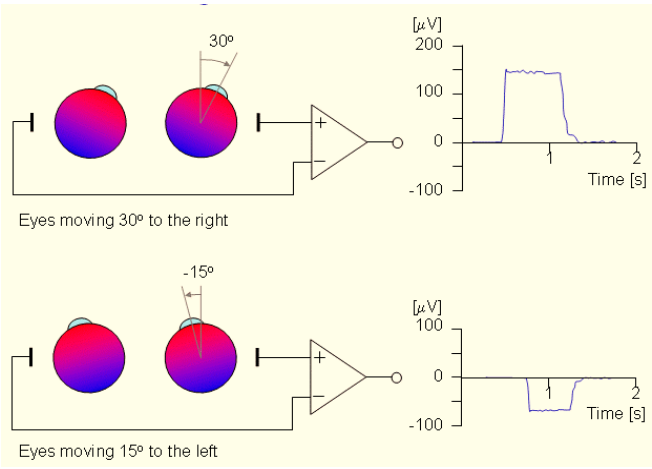

Figure 3.2: Horizontal EOG [2]

Vertical eye movement (vertical component) and blink are shown in figure 3.3.

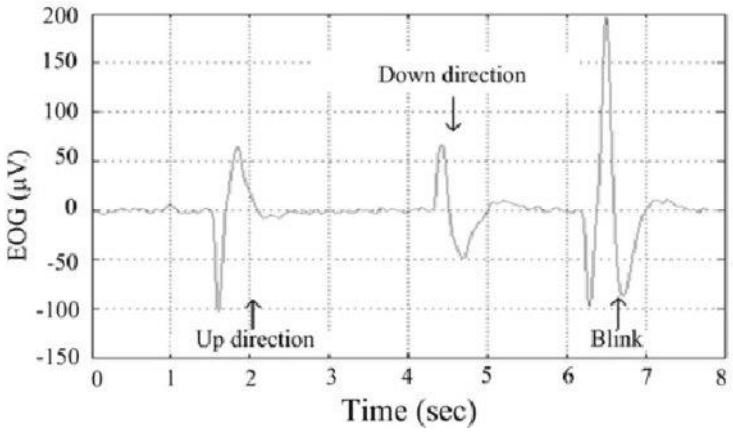

Figure 3.3: Vertical and Blink EOG

General block diagram for the EOG amplifier is shown in figure 3.4, it illustrates the filtration and amplification steps for the EOG signal. Firstly, an electrical background of the EOG signal will be discussed.

Figure 3.4: EOG amplifier block diagram

3.1.1 Surface Electrodes

An electrode is a medical device capable of transferring ionic current energy into electrical current in the body that can be amplified to treat as well as diagnose several ailments and life threatening conditions. EOG electrodes should be relatively non-polarizable such as standard medical electroencephalograph (EEG) or electrocardiograph (ECG) electrodes, of a size appropriate for attachment to the side of the nose.

Medical electrodes have several types as:

1) Micro Electrodes: this type is used during electrophysiology experiments to record electrical activity from neurons, but they can also be used to deliver electrical current into the brain or to neurons in culture in a process called microstimulation.

2) Needle Electrodes: . needle electrode. A fine wire through which electrical current may flow when attached to a power source; used to carry high frequency electrical currents that heat or destroy diseased tissue.

3) Surface Electrodes: Surface electrodes are those which are placed in contact with the skin of the subject in order to obtain bioelectric potentials from the surface as to get biomedical signal like ECG, EEG, and EOG.

Surface Ag/AgCl electrodes are the most common and favoured electrodes in clinical measurements for recording biological signals such as ECG, EMG and EOG. One of the main advantages of using Ag/AgCl electrodes is the low noise level it generates during biological signals recording. Ag/AgCl electrodes generate lower electrode-skin interface impedance and lower electrode-skin interface impedance value than stainless steel electrodes. They are also considered as non-polarizable electrodes; the non-polarizable nature of Ag/AgCl electrodes allows the charges to cross the electrode-electrolyte interface unlike stainless steel electrodes.

3.1.2 Pre-Amplifier

Pre-amplifier is a precision device have high input impedance, low output impedance, high common-mode rejection ratio, and low offset drift which is essential to get the micro-voltsignal, in this case, the EOG signal, figure 3.5 illustrates the schematic circuit of the pre- amplifier.

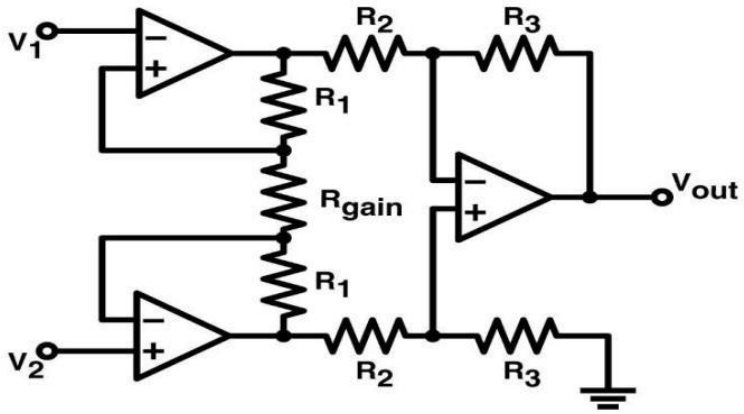

Figure 3.5: Pre-amplifier Circuit

AD620 is a low cost, high accuracy IC that requires only one resistor to set gain of 1 to1000, AD620 has 10G ohm input impedance, 100db common-mode rejection ratio and low output impedance which reduces the distortion of the signal, and with its wide power supply range (±2.3 - ±18 V) satisfies the signal pickup.

3.1.3 Filter

The signal collected from the electrodes is filtered using a fourth order Butterworth low pass filterwith a cut off of 30Hz to eliminate unwanted data.[3]

Butterworth filter is an accurate filter which passes the needed bandwidth; a higher orderproduces sharper bandwidth. The filter also offers amplification of 1.56 to the signal

AD822 IC consists of two cascaded amplifiers with ±1.5V to ±18V rail to rail supply, and with 1.6mA current consumption, it has a maximum offset voltage of 800µ volt and 2 µV/Co offset voltage drift. The minimum common mode rejection ratio is 74dB, and the typical one is 90dB .

3.2 Pressure Sensor

A normal human tongue pressure has from 3.2 to 52.4 Newton [4], person who has been paralyzed from the neck down and may not even be able to breathe on his or her own will still manage to move the tongue [5], also if with less pressure, the sensor can detect it.

There is several sensors calculate the force applied like FlexiForce A201 shown in figure3.9 [6], Xex761D shown in figure 3.10 [7], and FSR 406 shown in figure 3.11 [8].

Figure 3.9: FlexiForce A201 Pressure sensor

FlexiForce A201 actually is doesn't appropriate to be used in this project because of its high actuation force (about 4.4N) which will not sense the quadriplegic patient's tongue pressure.

Figure 3.10: Xex761D Pressure Sensor.

Figure 3.10 illustrates the Xex761D pressure sensor, Xex761D is a metallic sensor which cannot be mounted on the cheek, so can't be used in this project.

FSR406 shown in figure 3.11 is a thin layer sensor which easily can be mounted on the cheek; it has suitable dimensions to receive the force of the tongue from a wide area of the cheek, and actuation force of 0.1N which guarantees that it will receive the tongue pressure, FSR406 features are summarized in table 3.1.

Table 3.1: FSR406 pressure sensor characteristics.

Property	**Value**
Actuation force	0.1 Newton
Force sensitivity range	$0.1\text{-}10^2$ Newton
Stand-Off resistance	>10M ohm
Size	43.69 ×43.69 mm
Switch travel	0.05mm
Device rise time	<3 microseconds
Temperature operating range	-30 - +70 C^o
Number of actuations (Life time)	10 Million

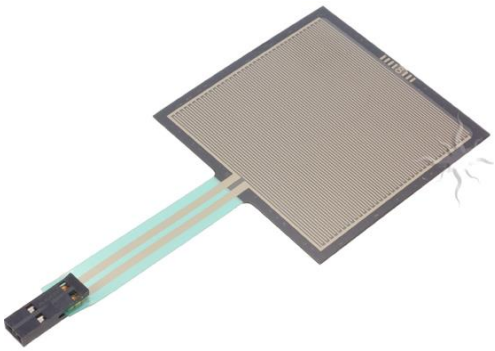

Figure 3.11: FSR406 Pressure Sensor.

Section 3.3 provides the theoretical background of the Arduino controller and their types. By the end of this section, an appropriate Arduino type should be chosen, and it will be clear what are the controller features does this project needs to achieve the wanted control.

3.3 Controller

The microcontroller receives the medical signal from the sensors circuits, and processes them. It takes the right decision of sending the signal to the next steps, Arduino controller is used to achieve this process.

Arduino is an open-source platform used for building electronic projects. Arduino consists of both a physical programmable circuit board (often referred to as a microcontroller) and a piece of software, or IDE (Integrated Development Environment) that runs on the computer, used to write and upload computer code to the physical board.

The programing language is used in the project is LabView, by a special toolkit; it will be compatible with Arduino hardware.

There are different versions of Arduino available which are: Arduino MEGA 2560, Arduino UNO, Arduino MINI, and Arduino NANO. Table 3.2 lights the main features of different Arduino versions.

Table3.2: Comparison of Different Versions of Arduino

Arduino version / **Feature**	**MEGA 2560**	**UNO**	**MINI**	**NANO**
Processor	ATmega2560	ATmega328P	ATmega328P	ATmega168 ATmega328P
CPU Speed	16MHz	16MHz	16MHz	16MHz
Analog I/O	16 / 0	6 / 0	8 / 0	8 / 0
Digital IO/PWN=M	54 / 15	14 / 6	14 / 6	14 / 6
Flash Memory (KB)	256	32	32	16 / 32
USB	Regular	Regular	-	Mini

Arduino UNO has an appropriate memory and digit/analog I/O pins, also it is available in the market with relatively cheap price, figure 3.12 shows the Arduino UNO controller and its pins.

Figure 3.12: Arduino UNO

Section 3.4 shows a brief explanation about electric motors with their types, at the end of the section, it will be clear what the specific types of motors does this project needs.

3.4 Motors

An electric motor (or electrical motor) is an electric machine that converts electrical energy into mechanical energy. Most electric motors operate through the interaction between the motor's magnetic field and electric current in a wire winding. This interaction generates a force (as per Faraday's Law) in the form of torque which is applied to the motor's shaft. [9]

Medical mobility equipment requires long life, high torque DC brush or brushless gear motors to achieve the long term performance and reliability that users expect.

3.4.1 DC Motor

A direct current (DC) motor is a type of electric machine that converts electrical energy into mechanical energy. DC motors take electrical power through direct current, and convert this energy into mechanical rotation. It has two major types; Brushed and brushless DC motors. [10]

A brushless DC motor is an electronically commuted DC motor which does not have brushes. The controller provides pulses of current to the motor windings which control the speed and torque of the motor. [11]

In a brushed DC motor, the rotor spins 180-degrees when an electric current is applied to the armature. In order to travel beyond the initial 180 degrees, the poles of the electromagnet must flip. Carbon brushes contact the stator as the rotor spins, flipping the magnetic field and enabling the rotor to spin 360-degrees. Figure 3.13 shows a general description for brushed and brushless DC motors

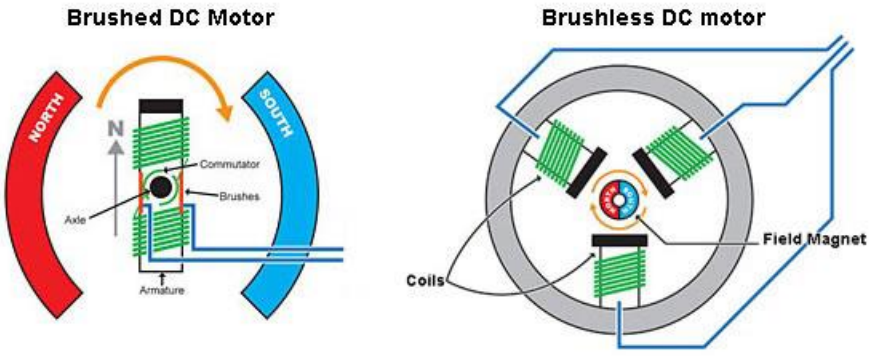

Figure 3.13: Brushed and Brushless DC Motors

3.4.2 Motor Driver

Driver is the interface between the controller and the motor; drivers are needed to supply the motor with enough voltage and current which can't be provided by the controller which gives a low-current signal to the driver.

When choosing a motor driver, some features must be taken into account, as the driver supply, its output voltage, number of output pins, how much current can stand with.

Motor drivers in general have four terminals on the input side, which are: supply, ground terminal, and two inputs for stop and control the direction of rotation. Figure 3.14 shows the type of motor driver we used .

Figure 3.14: 60A mos DC motor driver

3.4.3 Torque and speed

These two parameters are vital in wheelchairs to ensure safe and efficient drive ofthe wheelchair.

Torque is the twisting/turning force that causes rotation around an axis. In power wheelchairs this is a function of appropriate gearing of the gear box to assure the powerbase cannavigate obstacles effectively.

Most power wheelchair average a top speed of approximately 5 mph (about 8km/h). However,

some power chair models can achieve maximum speeds of 10 mph (about 16km/h) and more.

3.5 Power Switch

A power switch as shown in figure 3.15 is important to be used to connect/disconnect any supply for any component when needed.

When it is chosen, it must be taken into account how much voltage and current it can endure to avoid any failure.

Figure 3.15: Power Switch

3.6 Battery

The DC motor at wheelchair needs to feed 24V, so we connected two of the batteries of 12 batteries at series , and because the DC motor needs a high current and in order for work most time possible as possible so we want batteries with a high capacity ,and for that we use a battery with 94 AH, as shown in the Figure 3.16.

Figure 3.16: 12V 94Ah battery

And because the current coming from the wheelchair battery feeding is high and to increase the safety of the patient, the EOG circuit was separated with two other batteries with a power of 12 so that we could get a supply of 12 and -12, and a current capacity of 1.3, so that it could supply the special circuit EOG, and also the Connect it to a protection switch for use when needed. as shown in the Figure 3.17.

Figure 3.17: 12V 1.3Ah battery

Chapter Four

System Design

This chapter illustrates the overall project's design including the hardware components to achieve the desired purpose; creating safe, effective, and low cost eye-controlled wheelchair fulfill the needs for people with quadriplegia.

4.1 EOG System

As known, EOG signal is produced by eye movements, it is the potential difference between cornea and retina, acquiring an accurate EOG signal will make accurate eye-gaze detection.

This section illustrates how does the EOG signal will be processed to obtain the pure EOG signal, Figure 4.1 shows the stages of processing the EOG signal.

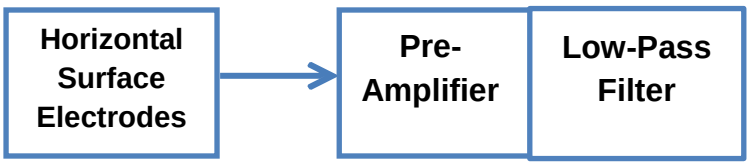

Figure 4.1: EOG System Block Diagram

Another Block diagram of the same stages will be done for Vertical EOG signal processing, then, the two processed EOG will be stored in the Arduino controller.

Arduino can receive analog input voltage of maximum 5 V, with EOG amplitude range of 100-3500 µV, the overall amplification must be 1143 to have maximum output from the EOG system with 4V.

4.1.1 Surface Electrodes

The mechanism of electric conductivity in the body involves ions as charges. Picking up bioelectric signals involves interacting with these ionic charges and transuding ionic currents into electric currents required by wires. This transuding function is carried out by electrodes that consist of electrical conductors in contact with the aqueous ionic solutions.

(Ag-AgCl) electrode –shown in figure 4.2- are used in this project for their high sensitivity and high accuracy of detecting signals .In this project the electrodes will be put in fifth different places to detect the

electrical signal from eyes muscle .One of these electrodes are put above the eye and the other under the eye, the other two electrode will be put it in the left and on the right around the eye. The fifth electrode will be used as reference.

Figure 4.2: Ag/AgCl Electrodes.

Right and left electrodes pick up the horizontal eye movement EOG signal which make the horizontal channel, meanwhile, the up and down electrodes pick up the vertical eye movement EOG signal which make the horizontal channel. The fifth electrode will set as reference, figure 4.3 shows the vertical and horizontal channels.

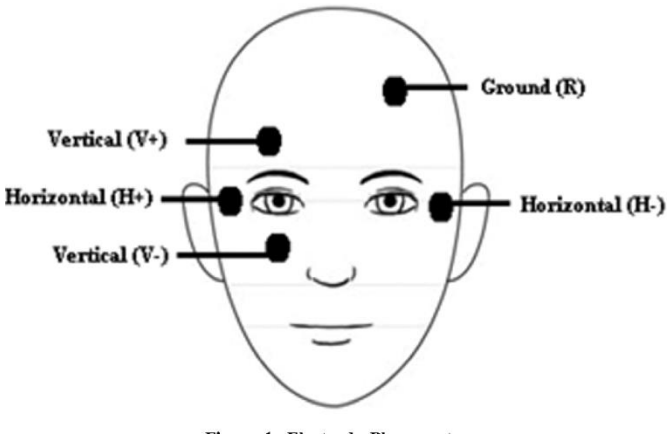

Figure 4.3: Horizontal and Vertical Channels.

4.1.2 Pre-Amplifier

As explained, EOG amplitude is between [100-3500]μV, according to this low amplitude, it needs an accurate filtering and amplifying.

AD620 with its high accuracy, low offset voltage of 50μV, and offset drift of 0.6 μV/C^{o} is ideal to be used in precision data acquisition systems such as this project; EOG acquisition.

AD620 IC will be used with RG= 5.6kΩ calculated according to equation 4.1 to get gain = 10. Figure 4.4 shows the schematic to the AD620, whereas RG is connected to the pins 8 and 1.

$$Av = \frac{49.9k}{RG} \qquad (4.1)$$

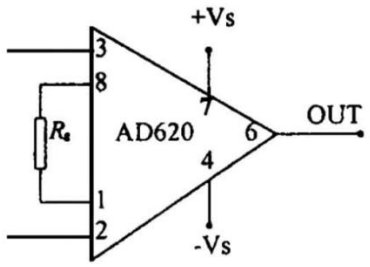

Figure 4.4: Pre-Amplifier Circuit

4.1.3 Butterworth Low Pass Filter (LPF)

The output signal from the instrumentation amplifier is the input for the Butterworth 4th order LPF, which is used to hold the required frequency bandwidth under 30Hz, the 4th order LPF is designed by implant two 2nd order low pass filter respectively, in which the output of the first one is the input for the second.

AD822 IC is used to design the LPF, it consists of two cascaded amplifiers as shown in figure 4.5, each amplifier is used as 2nd order low pass filter for its high common mode rejection ratio of 80dB, and offset drift of 2 micro volt /C°

$$fc = \frac{1}{2*\pi*R*C} \quad \ldots . 4.2$$

$$AV = 1 + \frac{Rf}{Rin} \quad \ldots . 4.3$$

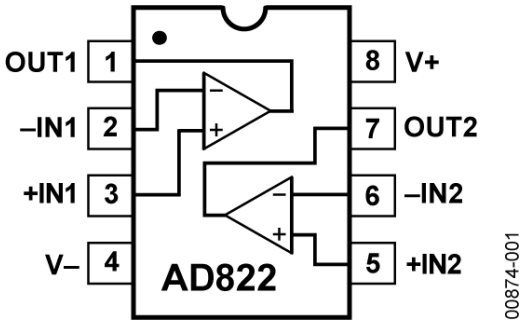

Figure 4.5: Internal Circuit for AD822

Using equation 4.2 with fc = 30 Hz for the LPF, and assuming C1=C2=C3=C4= 220 nf; the resistors values R2=R3=R6=R7= 24kΩ.

To achieve Butterworth filter, the gain must be 1.5 for each amplifier, using equation 4.3, and assuming R5=R9=10kΩ, and R4=R8= 15kΩ as shown in figure 4.6.

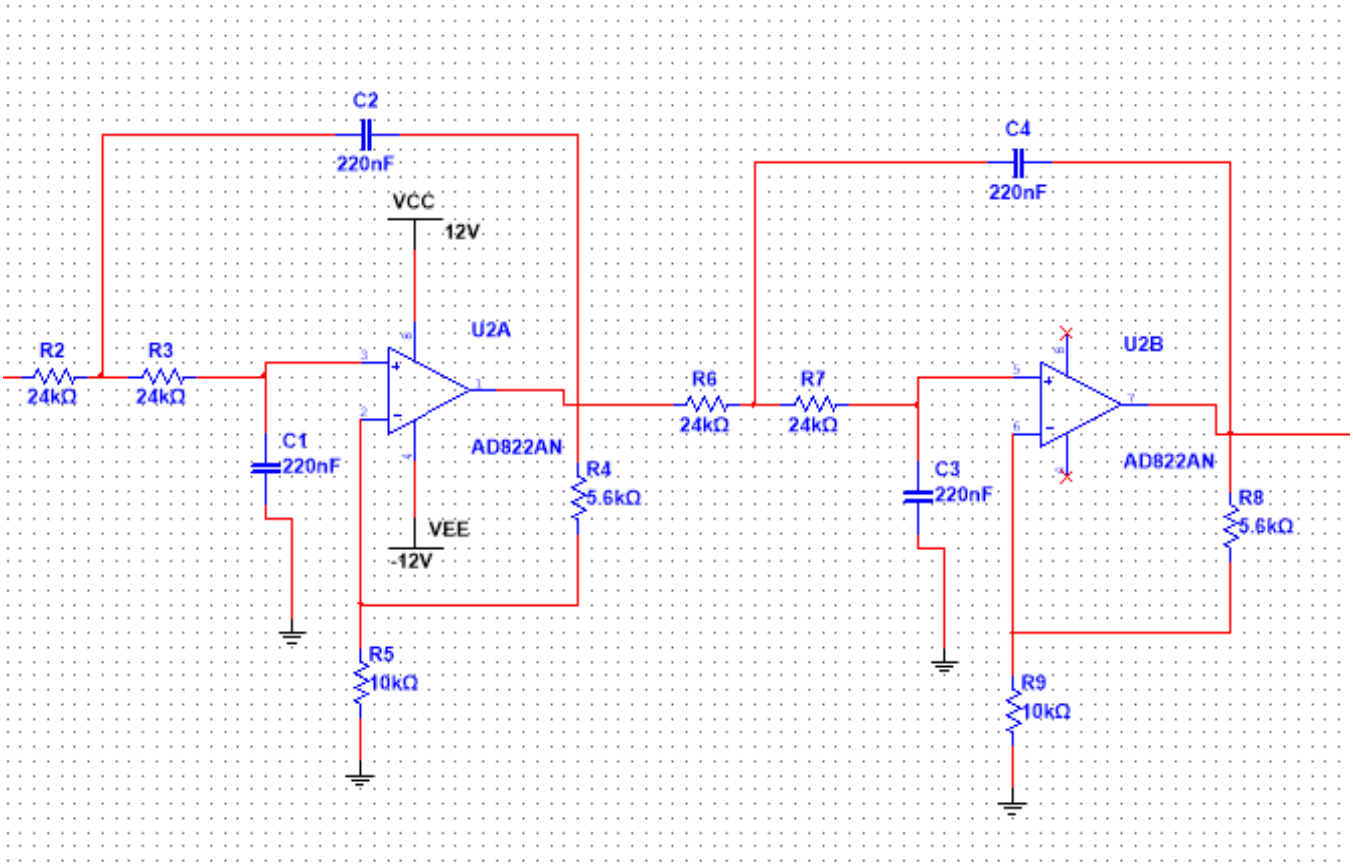

Figure 4.6: 4th order low pass filter.

4.1.4 Overall EOG system Circuit

The overall system consists of two circuits, one for horizontal gazing, and the other for vertical gazing, which contains the input from the EOG electrodes to the instrumentation amplifier, and the fourth order Butterworth low pass filter which gives the filtered EOG signal to the Arduino, Figure 4.7 illustrates the overall EOG circuit.

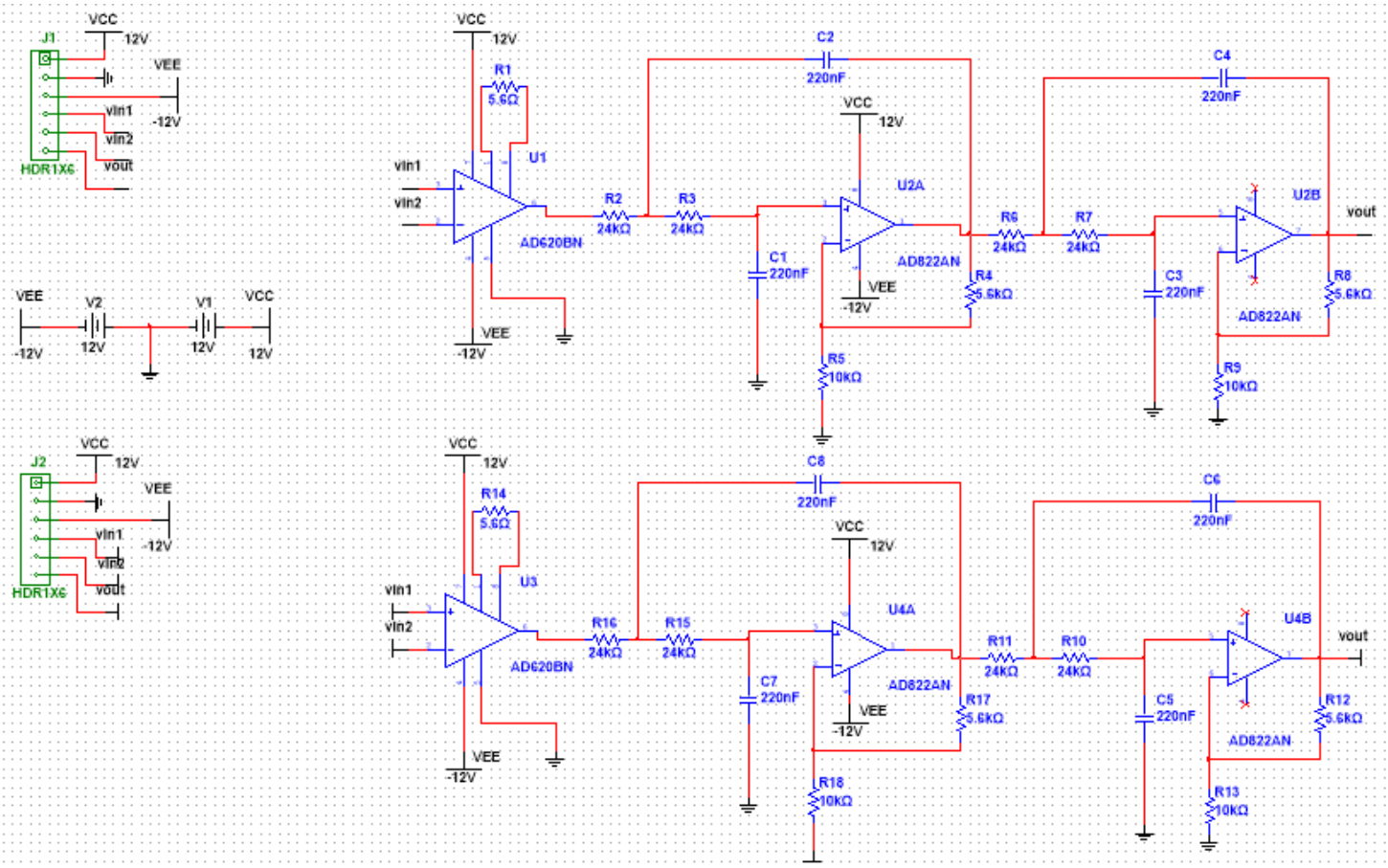

Figure 4.7: Overall EOG system

4.2 FSR406 FlexiForce Sensor

The FSR406 FlexiForce sensor will works in parallel with the EOG system and its signal will be sent to the Arduino, it will be connected with the controller with resistor Rm which is used to limit the current. Figure 4.8 shows the equivalent circuit for the pressure sensor.

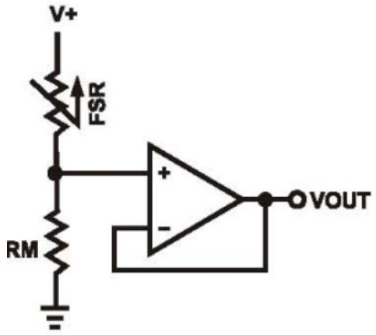

Figure4.8: Equivalent Circuit for the Pressure Sensor

The output voltage from the pressure sensor is derived by equation 4.5. Figure 4.9 illustrates the variations of the output according to the variation in Rm with $^{+}$5V supply.

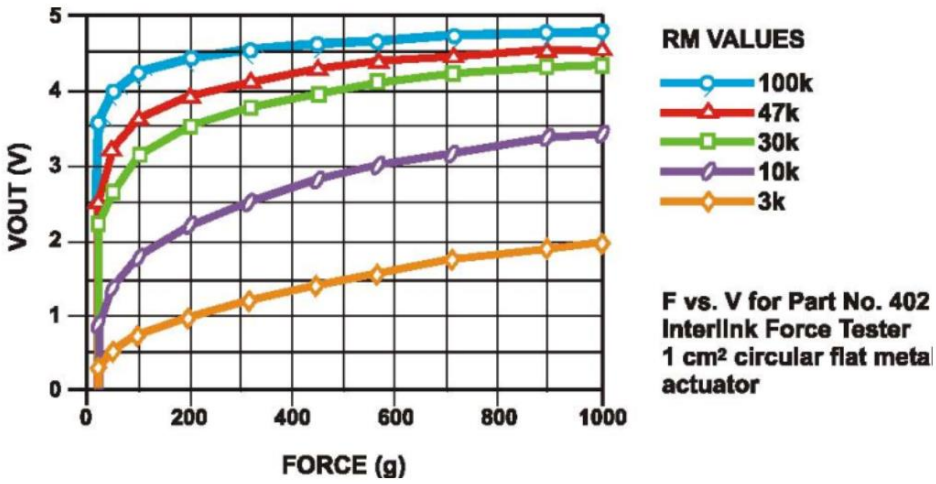

Figure 4.9: FSR406 Output Voltage and Force Due to Changes in Rm

$$Vout = \frac{Rm * V+}{Rm + Rfsr} \qquad (4.5)$$

Table 4.1 shows the variations of Rfsr with variation in pressure force. With minimum tongue force of 3.2N [5], and due to equation 4.4, to achieve output voltage appropriate to Arduino which is less than 5V, 3k ohm with 12volt supply.

Table 4.1 variation of FSR Resistance Due to the Applied Force [6]

Force (N)	**FSR Resistance**
None	Infinite
0.2	30 k ohm
1	6 k ohm
10	1 k ohm
100	250 ohm

Figure 4.10 shows the pre-processing circuit.

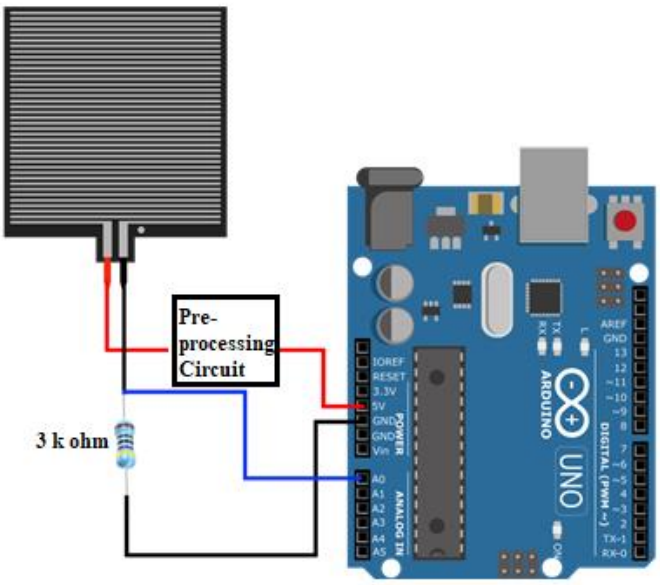

Figure 4.10: FSR406 Pressure Sensor Circuit

4.3 DC Motors

DC motor is responsible for the forward, backward, turning right, and turning left according to the coming signal from the controller after EOG analyze.

The used DC motors are the motors of the Puma40 electrical wheelchair which consumes 74Ah, the motors are supplied by 24 volts by two 12 volt chargeable batteries connected in series, with 92.8Ah current supply, and maximum speed of 10km/h, figure 4.10 shows the technical information for the Puma40 DC motors.

7.2 Technical information

Batteries	Max.	Unit
Maximum battery dimensions	260 x 172 x 210 (10.2 x 6.8 x 8.3)	mm (inch)
Maximum battery dimensions with Dahl system	260 x 172 x 190 (10.2 x 6.8 x 7.5)	mm (inch)
Battery capacity	40 / 60 / 74 GEL; 50 AGM (Puma 20 only)	Ah
Battery capacity with Dahl system	40 / 60	Ah
Maximum permissible charging voltage	24	V
Maximum charging current	12	A (rms)
Connector type	Controller	
Insulation Class 2 double insulated	Class 2 double insulated	

Figure 4.10: Technical information for the DC motors

To acquire the desired current and voltage to the motors, drivers are used; section 4.4 explains more about the used motor Driver.

4.4 MOS Dual Channel H-bridge DC Motor Driver

This module is super wide voltage motor driver; it can achieve 48Volts with 60A current, and can control two motors as shown in figure 4.11, some of its features:

1- It has built-in 2 channel high power DC motor drive.
2- Small size: 70mm * 56 mm.
3- Good heat sink to keep good performance.
4- Control interface is very simple: A1, A2 = 0.0 for brake; A1, A2 = 1.0 for forward; A1, A2 = 0.1 for Reverse.PA for PWM wave input (motor speed regulation); G for common Ground (B channel for the same control).
5- All MCU of 3.3 V and 5 V are can control this module, and only need one channel motor power

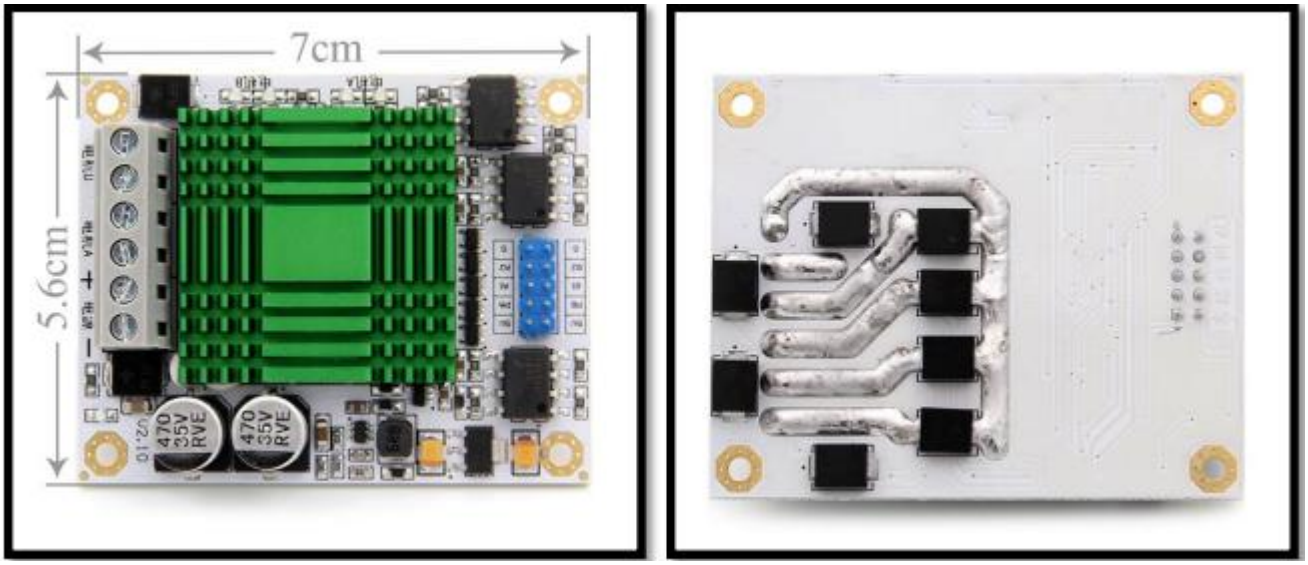

Figure 4.11: MOS Dual Channel Motor Driver.

Figure 4.12 shows a detailed explains for the driver pins.

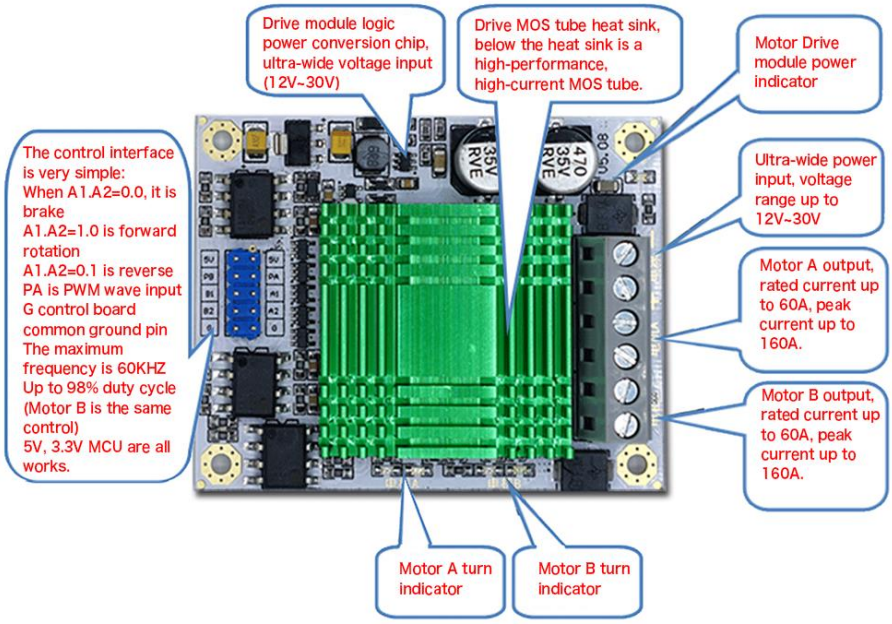

Figure 4.12: Detailed Explain for the Driver

4.5 Power Supply

In this project, a 12V battery will be used to supply the system; table 4.2 shows thecurrent consumption of the system components.

Table 4.2 Current Consumption of the System.

Component 'sName	Number of Pieces	Quiescent Current
AD620	2	2.6mA
AD822	2	3.2mA
Arduino At UNO	1	1.5mA
Total Quiescent Current		7.3mA

4.6 Overall system Circuit

in this section we simulate the circuit between the EOG signal and the FlexiForce sensor with the wheelchair , Figure 4.13 show the system circuit

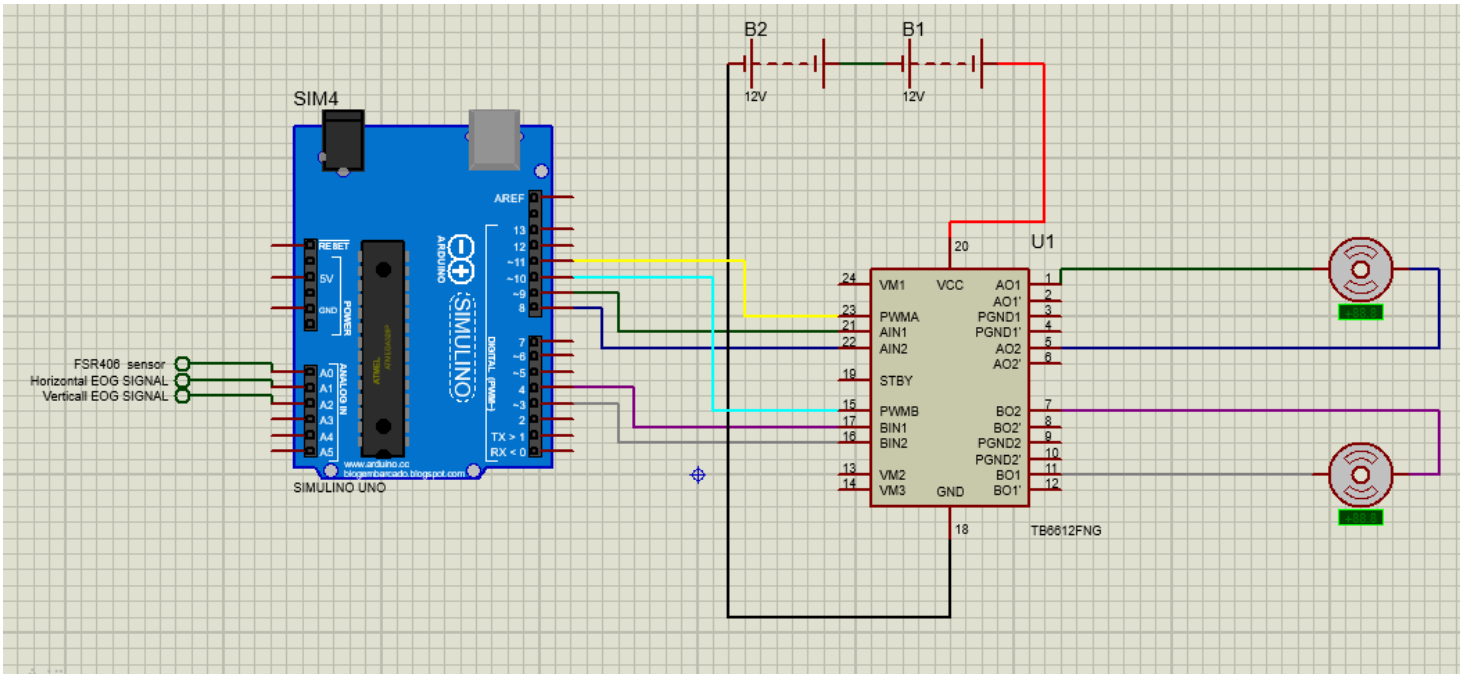

Figure 4.13: system Circuit

4.7 Flow Charts

In this section, flow charts will clear the operating procedure for both eye controlling system and the FlexiForce sensor to control the wheelchair. Figure 4.16 show the pressure sensor flow chart in the project.

Figure 4.14 illustrates the flow chart of the horizontal eye-controlling system, whichmoves the wheelchair right and left.

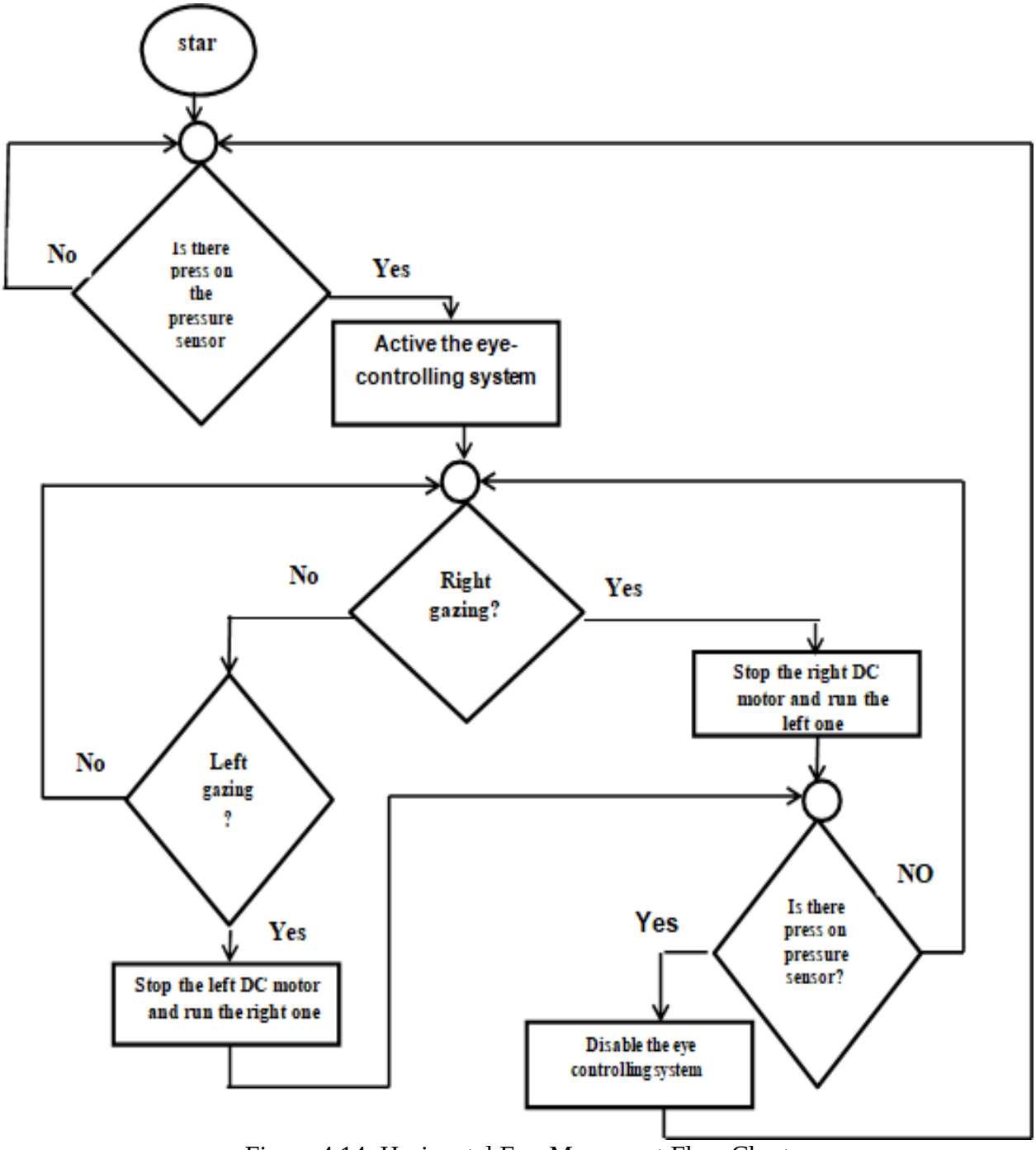

Figure 4.14: Horizontal Eye-Movement Flow Chart

Figure 4.15 shows the flow chart for the up gazing.

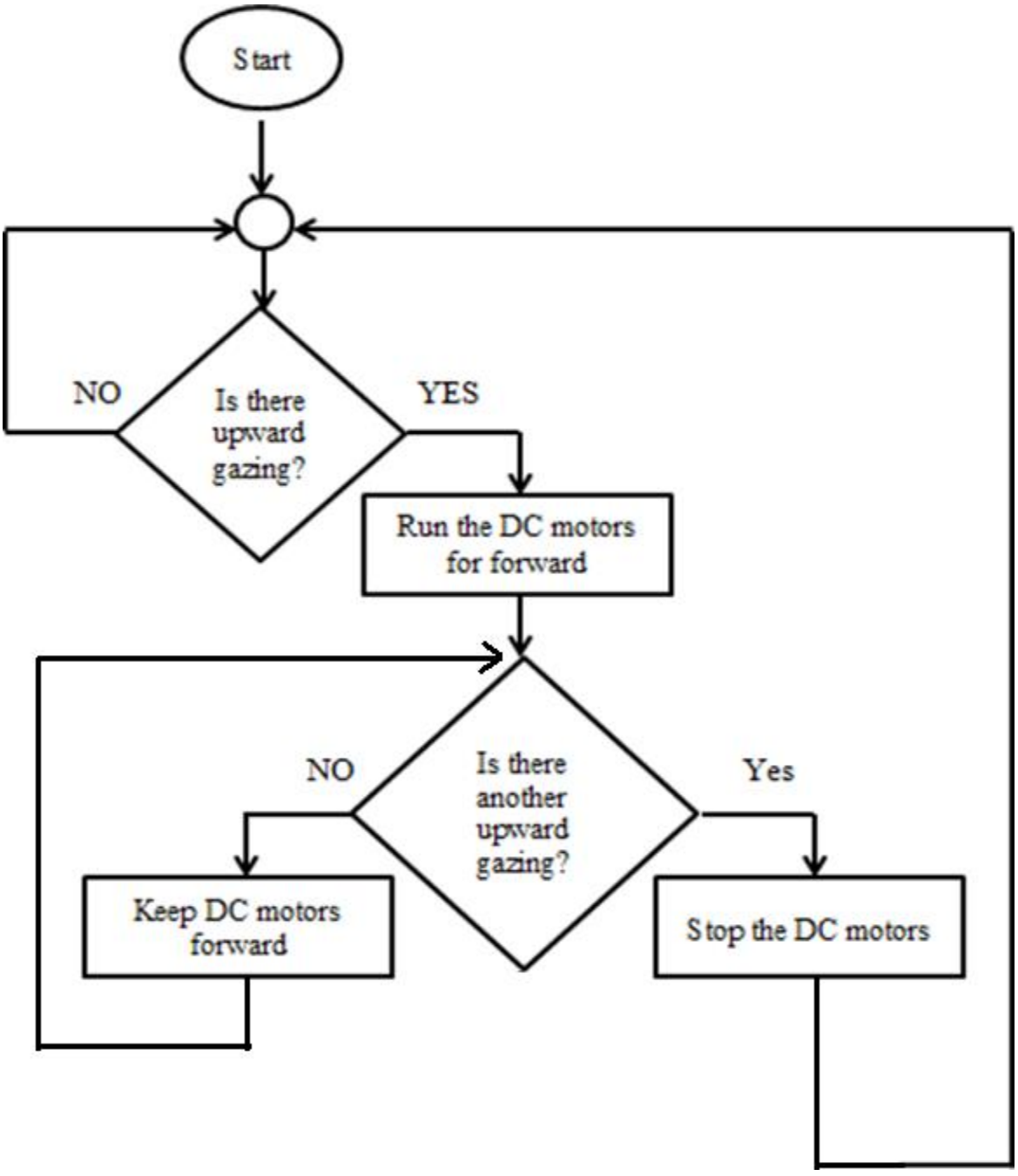

Figure 4.15: Upward Gazing Flow Chart

Figure 4.16 shows the flow chart for the FSR406 pressure sensor.

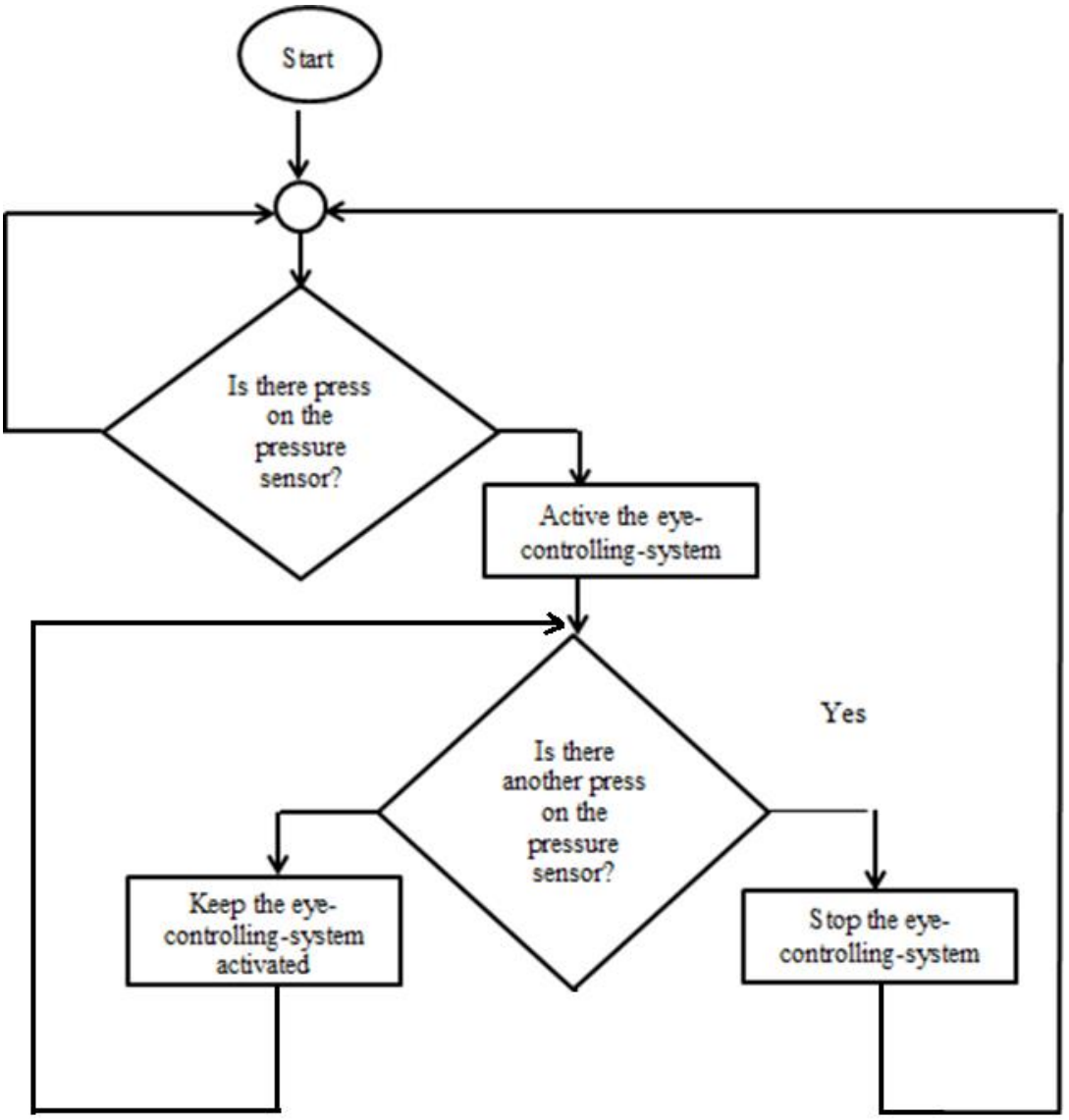

Figure 4.16: Flow Chart for the Pressure Sensor.

Chapter Five

Testing and Results

5.1 Overview

In this chapter, the results of testing the systems are shown; EOG Circuit, FelxiForce sensor, and the overall system combined with the motors.

5.2 EOG System Tests

In this section, the testing results of the EOG circuit components will be illustrated and discussed.

5.2.1 Fourth Order Low Pass Filter Testing

A fourth order LPF with gain=1.56 and critical frequency of 30Hz is used to achieve sharper filtration of the signal by increasing the order, it designed using ad822 IC, figure 5.1 shows the output of the filter with 1 volt AC input at 30 Hz, which amplified to be 1.6V.

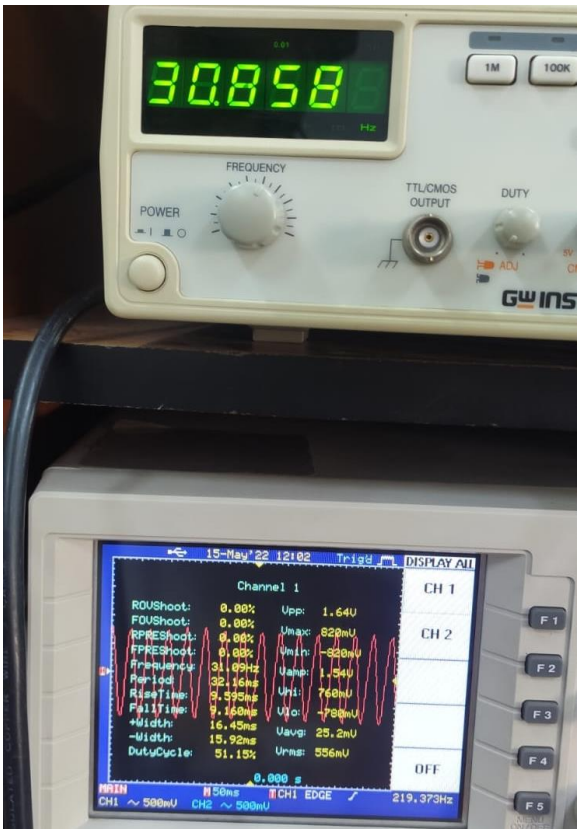

Figure 5.1: Output From the 4th Order LPF at 30 Hz.

Figure 5.2 shows the output of the filter with the same input voltage at 50 Hz, which shows the decaying of the input at this frequency to 600mV which represents the noise signal.

Figure 5.2: Output From the 4th Order LPF at 50 Hz

Table 5.1 shows the output voltages with 1V AC input at different frequencies.

Table 5.1: Output Values From the 4th Order LPF at Several Frequencies.

Frequency (Hz)	**11**	**20**	**30**	**45**	**50**
Output Value (Volt)	2.3	2.16	1.64	700m	600ml

5.2.2 Horizontal EOG Test

EOG circuit is designed to give the EOG signal values for gazing right and left with amplitude between 0-5 volts to be suitable as input for the Arduino, Figure 5.3 shows the EOG circuit design which is tested on breadboard.

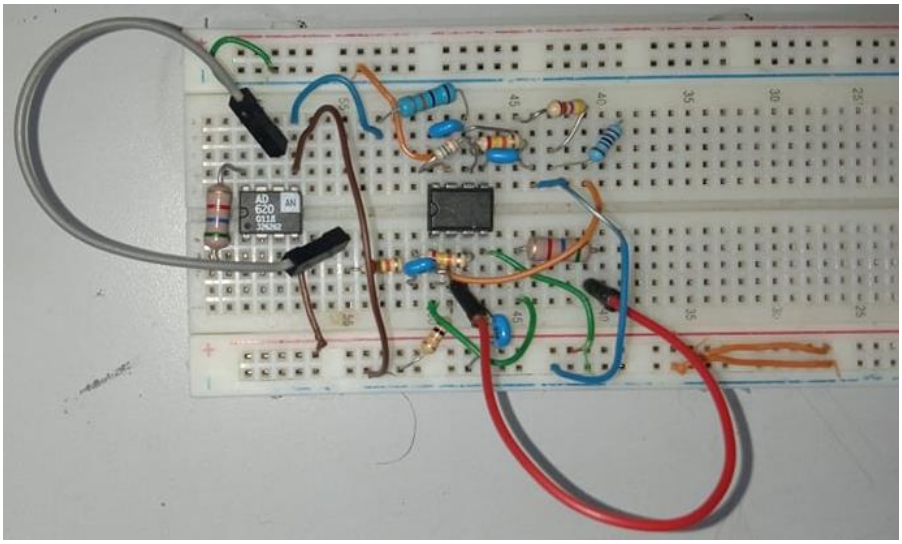

Figure 5.3: EOG Circuit on breadboard.

Circuit shown in figure 5.3 gave an output between 0-5 volts and stored in LabView code using Arduino, table 5.2 shows the output EOG values at gazing right.

Table 5.2: EOG Output for Gazing Right.

EOG output (Volt)	3.3	4.3	4.1	4.4	4.54	4.33	4.39	4.4	3.6

Table 5.3 shows the EOG output for gazing left.

Table 5.3: EOG Output for Gazing Left.

EOG output (Volt)	1.64	1.65	1.66	1.67	1.5	1.10	1.11	0.26	0.7

Figure 5.4 shows the output values from the EOG circuit in LabView software.

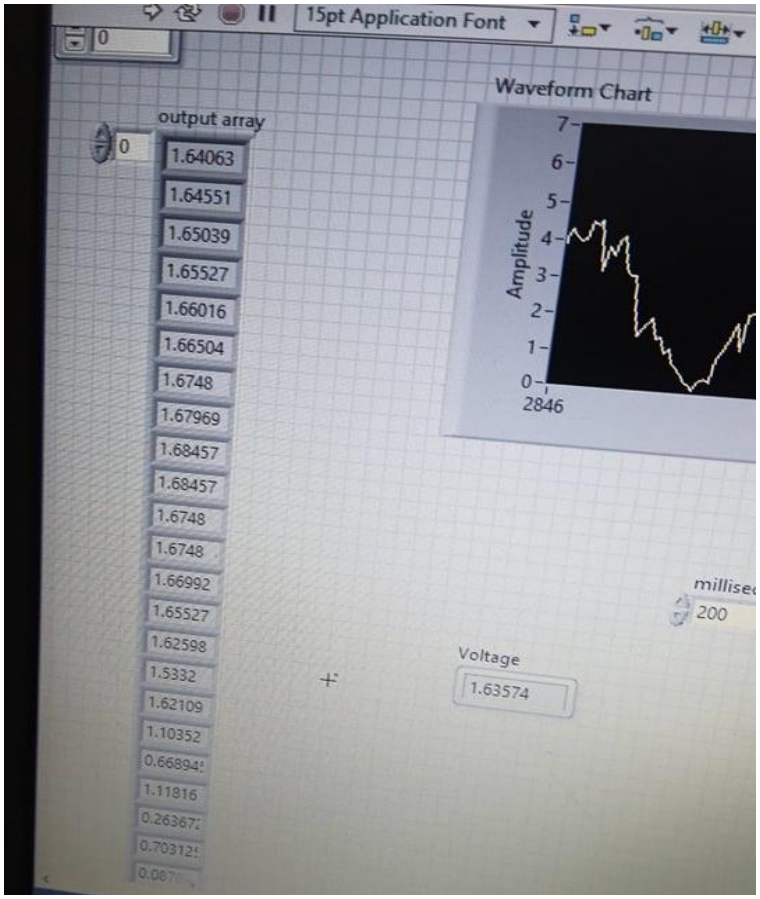

Figure 5.4: Output Values From the EOG Circuit

Figure 5.5 shows the other values for moving eyes from left to the right, where the values can be seen in rising.

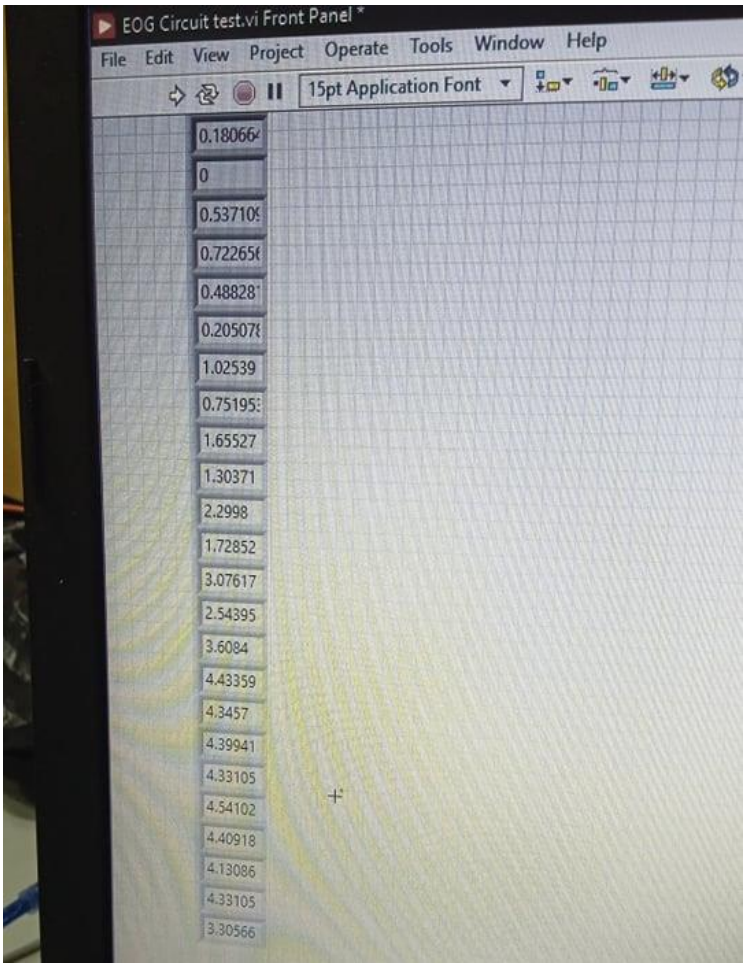

Figure 5.5: Output Values From the EOG Circuit while moving eyes from left to the right

The output voltages illustrated the main feature of the EOG signal for gazing right and left; EOG for gazing right gives values greater than gazing left, so by using value of 2.5 as reference, any value lower than it represents gazing left, and any value more than it represents gazing right, it is important to know that the output values for the EOG signal been read by the Arduino immediately when the eye moved, which make an excellent time response for the eye-controlling-system.

In order to make more accurate system, the circuit is designed on PCB; because PCBs have less noise and the electronic components will be fixed more on it. Figure 5.6 shows the design of the EOG circuit using Ultiboard software to print it as PCB.

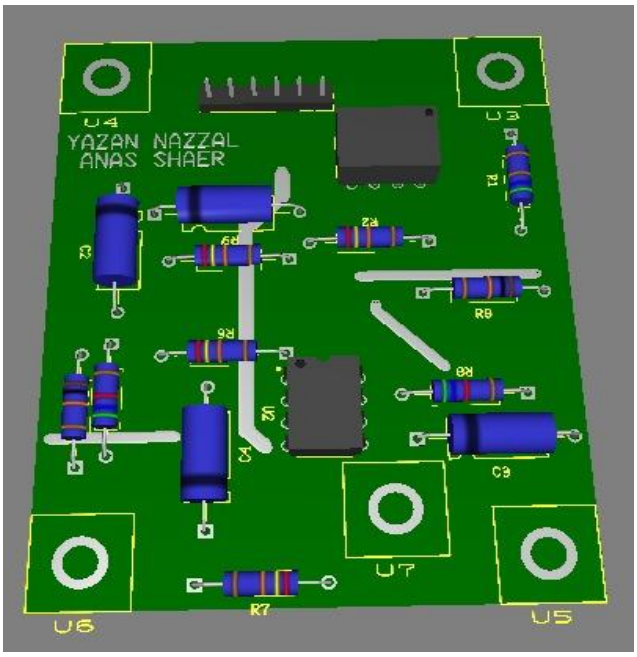

Figure 5.6: Design EOG Circuit in Ultiboard Software.

Figure 5.7 illustrates the EOG circuit on PCB board.

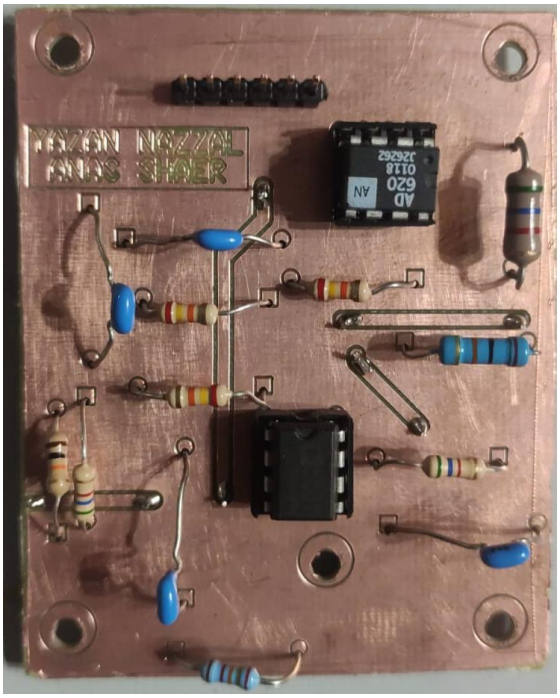

Figure 5.7: EOG Amplifier and Filter Circuit on PCB Board

Section 5.3 explains the testing and results of the FSR406 FelxiForce sensor.

5.2.3 Eye-Driving-System Code

Figure 5.8 shows the code for the system, which will control the two DC motors according to the gazing direction which is decided by the value of the EOG signal.

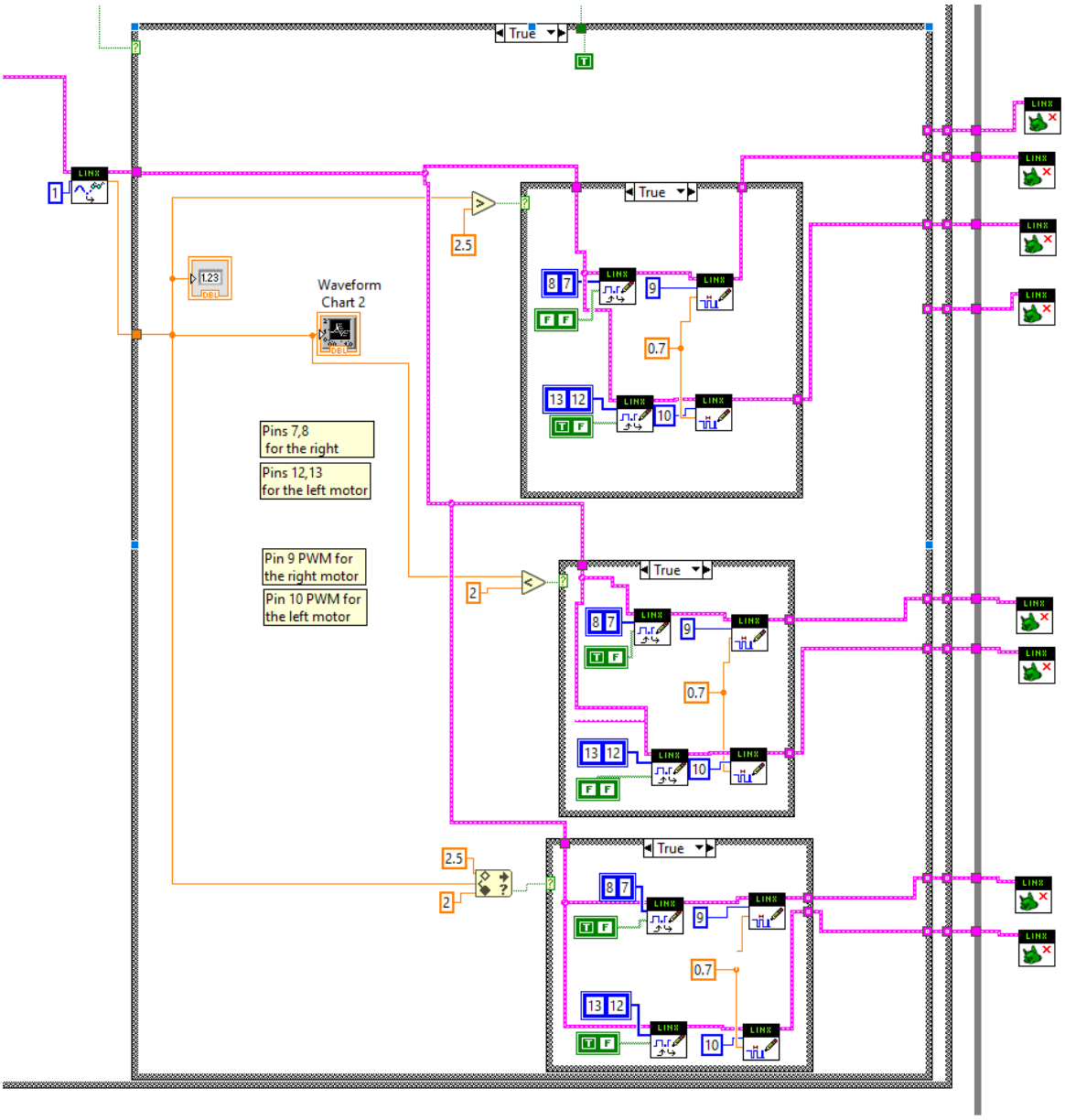

Figure 5.8: Eye-Driving-System Code

Running this code is conditioned by getting a value from the FlexiForce sensor over than 1.5. When it activated, a comparison will be done for the EOG value to decide the direction of the eye gazing, then, the signal will be sent to the motors; at right gazing, the right motor will be stopped and the left one will be activated, for left gazing, the opposite will be done, for if the user want to go back; he/she can rotate the wheelchair 180^{o} by gazing either to the right or the left.

The second press on the sensor will send zero as a reading for the sensor, which makes the condition false, in this case, the eye-controlling-system will be deactivated, and the two DC motors will move forward. Figure 5.9 illustrates the code for this case.

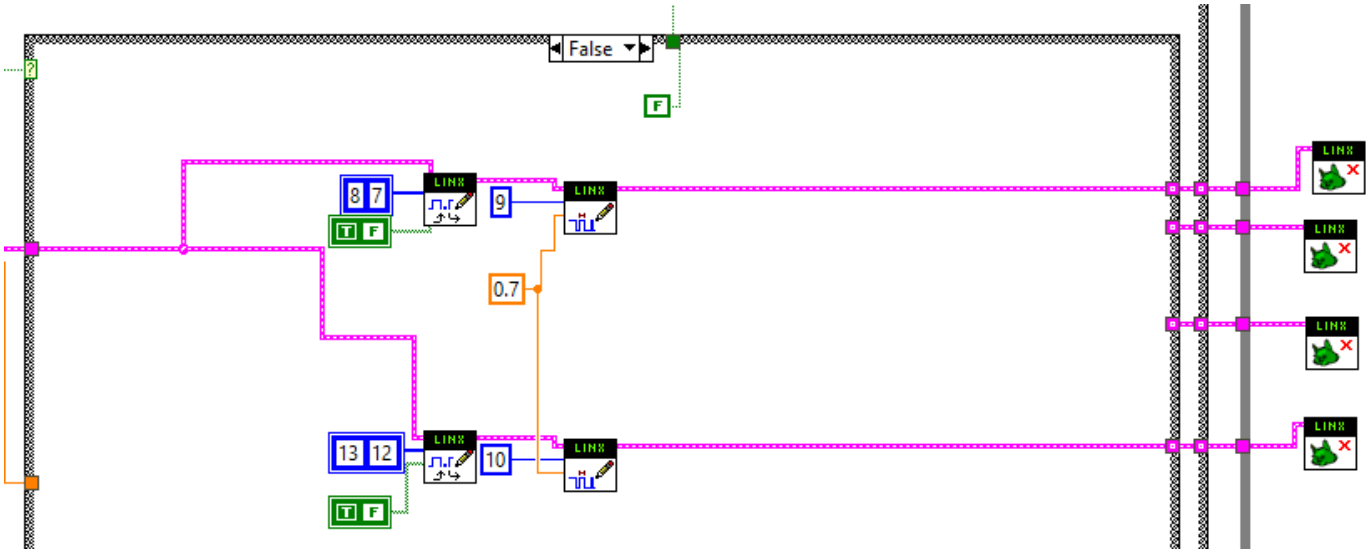

Figure 5.9: False Case for the Eye-Driving-System

5.2.4 Vertical EOG Analyzing

As shown in figure 3.3 in chapter three, the EOG signal for the vertical eye movement is distinguished by the increasing and decreasing rhythm, it decrease, then increase, then decrease, so the derivative of this signal will be negative, then positive, then negative, if this rhythm detected; the two DC motors will be stopped, otherwise, the motors will move forward, so the user can break the wheelchair by looking forward. It is important to know that the vertical EOG code is note conditioned by the FSR406 output; it is activated all the time

.

Figure 5.10 shows the vertical EOG analyze code, and the case of true which is means that there is an upward gazing.

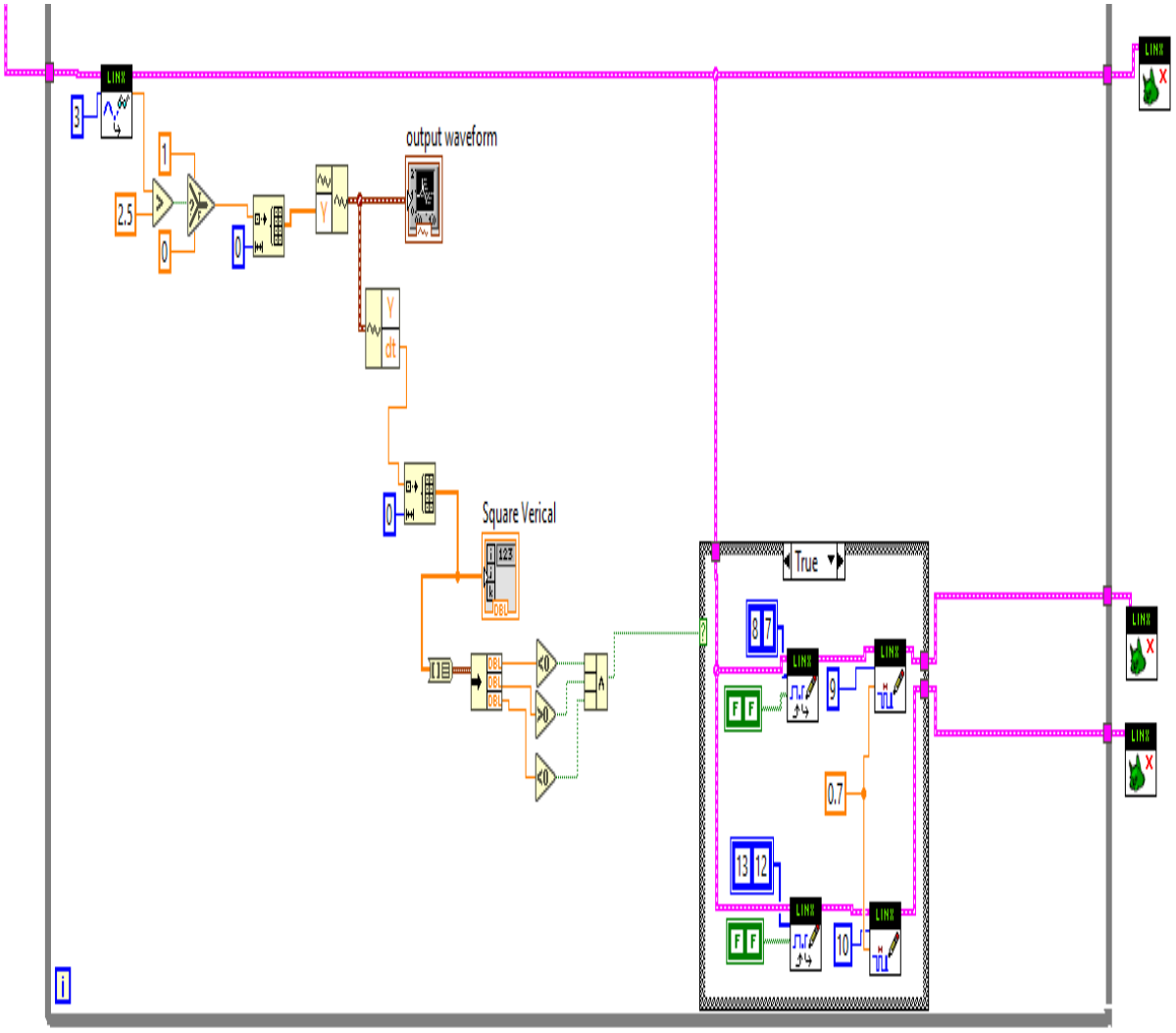

Figure 5.10: Vertical Gazing EOG Code, and Case True.

Figure 5.11 illustrates the false case which means that there is no upward gazing.

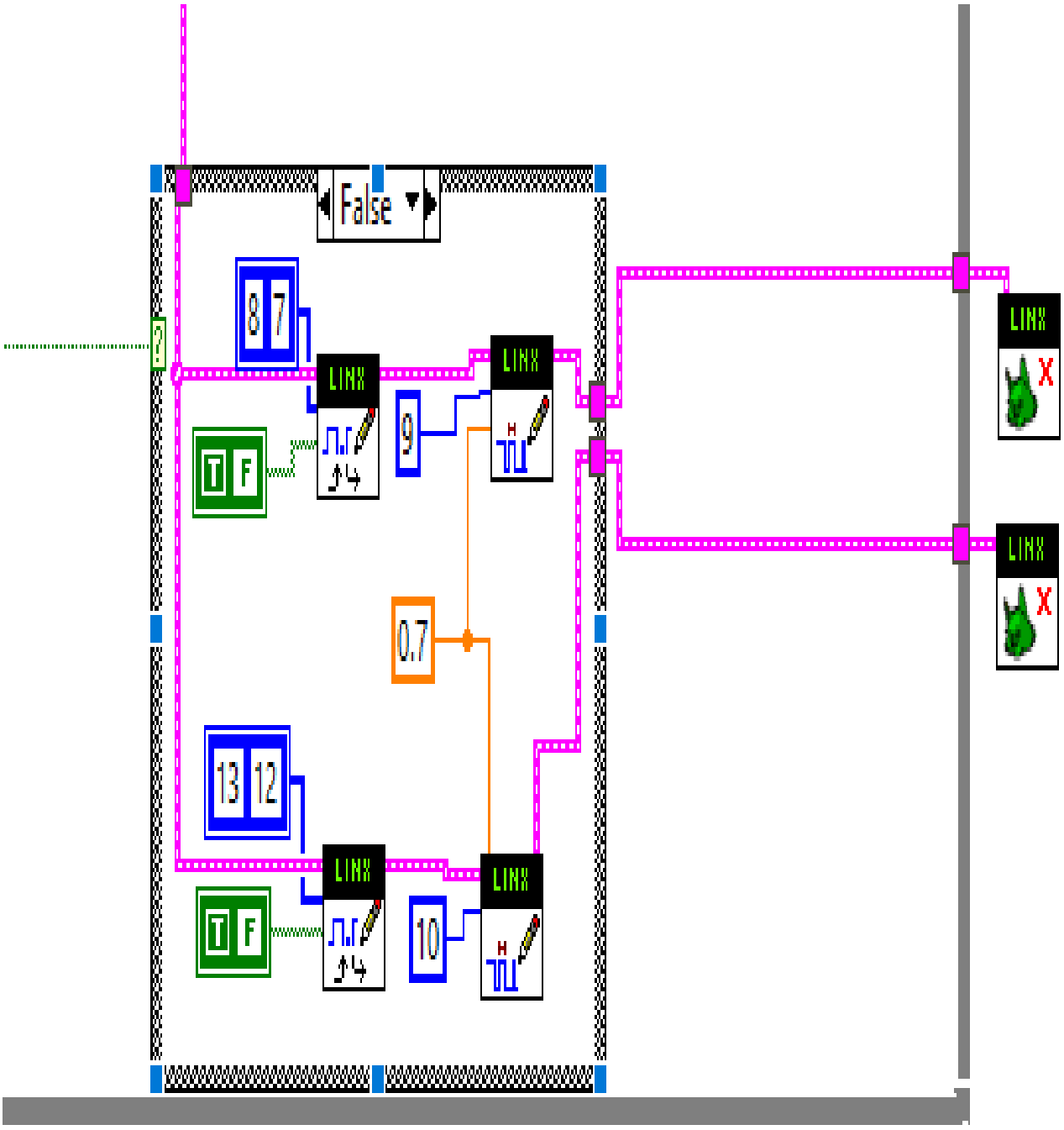

Figure 5.11: False Case of Vertical EOG

5.3 FSR406 FelxiForce Sensor Test

Flexiforce sensor is used as a switch for the eye-driving-system; to let the user turn on the system just when it needed, and look freely otherwise. Figure 5.12illustrates the result when a press is done on the pressure sensor, where the LED represents the running the eye-driving-system.

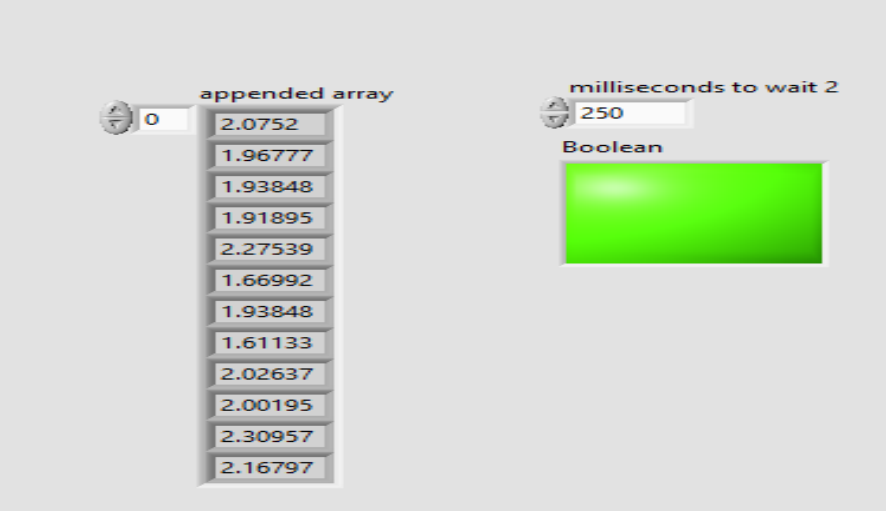

Figure 5.12: Press on the FlexiForce Sensor

The values in the array are the values came from pressing on the FlexiForce sensor, where the first value is compared with the threshold of 1.5, if exceeded, the case will be true and the eye-driving-system will be activated-which is represented as LED for testing-.

Figure 5.13 shows the result of other press on the sensor, which will send value of 0 to the first box of the array which is less than the threshold, so the case will be false and the eye-driving-system will be deactivated.

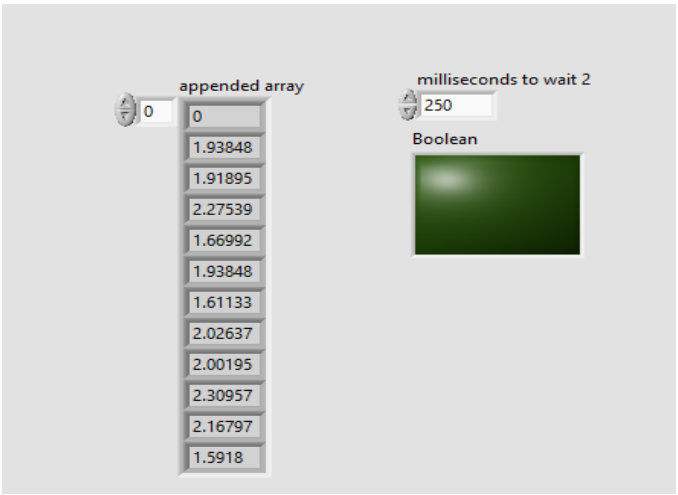

Figure 5.13: Second Press Result.

Figure 5.14 shows the code which will get the readings of the FelxiForce sensor, compare it with the threshold, and then inter it to an array, and the next press will inter zero.

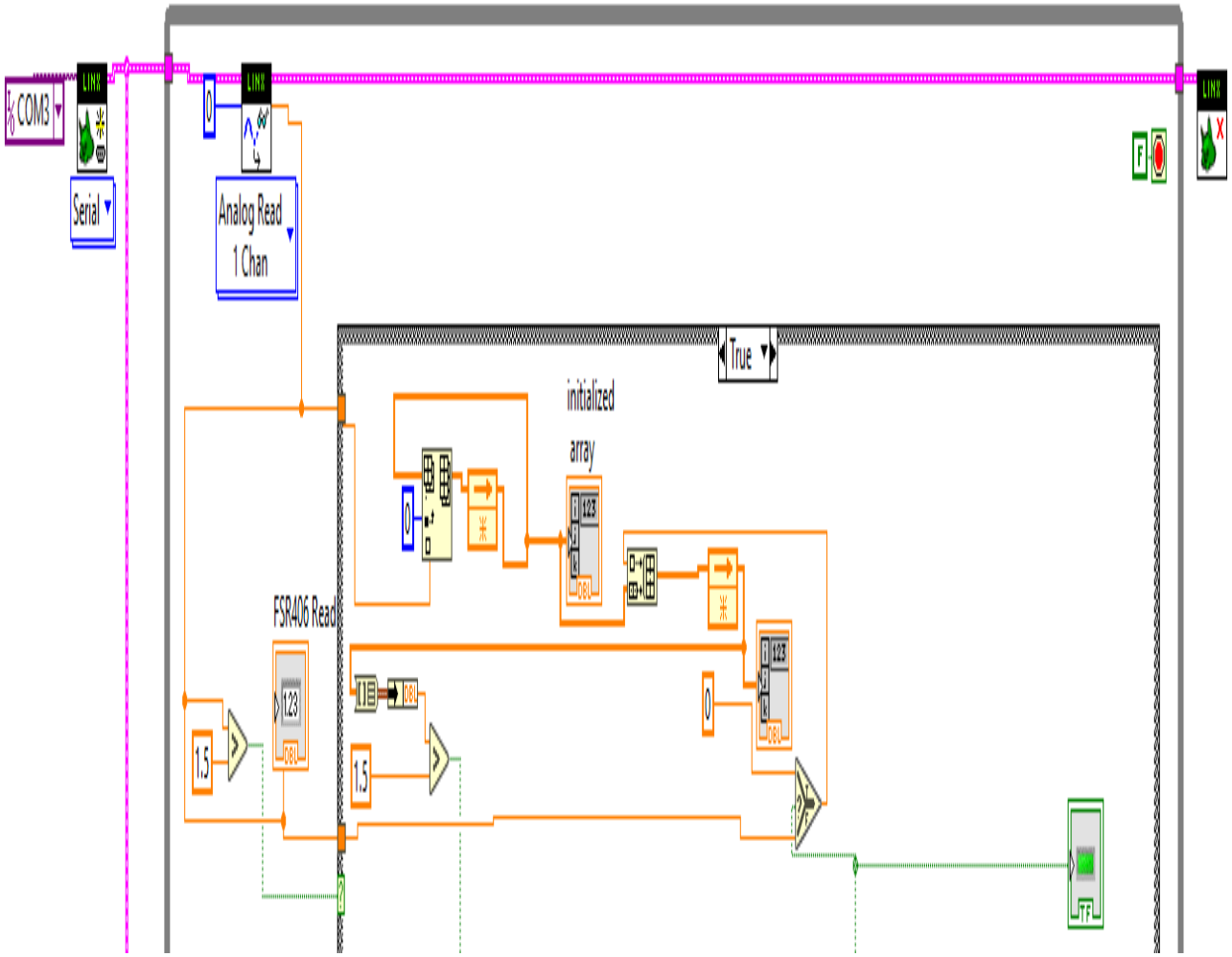

Figure 5.14: FSR 406 FlexiForce Sensor Code.

5.4Switching System

For more safe usage, a switching system is designed, it will be explained in this sections

5.4.1 Power Switches

A switches are designed between the wheelchair and EOG circuits batteries, and the other systems; to decrease power consumption, figure 5.15 shows the two switches; the bigger for the wheelchair battery, which stands with more current up to 20A, and the smaller one for the circuits battery which stands with current up to 4A.

Figure 5.15: EOG Circuits and Wheelchair Battery Switches.

5.4.2 Driver Switches

The wheelchair has a built-in driving system, instead of delete it, a switches are designed in order to switch between it and the eye-driving-system. Figure 5.16 shows the drivers' switches.

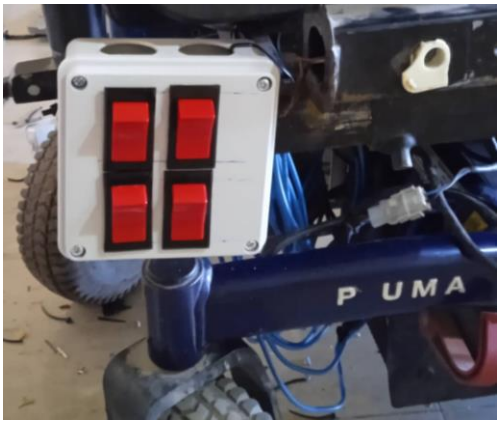

Figure 5.16: Drivers Switches

The upper switches for the Eye-driving-system, and the lower ones for the wheelchair driving system.

5.5 System Code

Figure 5.17 shows the overall code in cases of True.

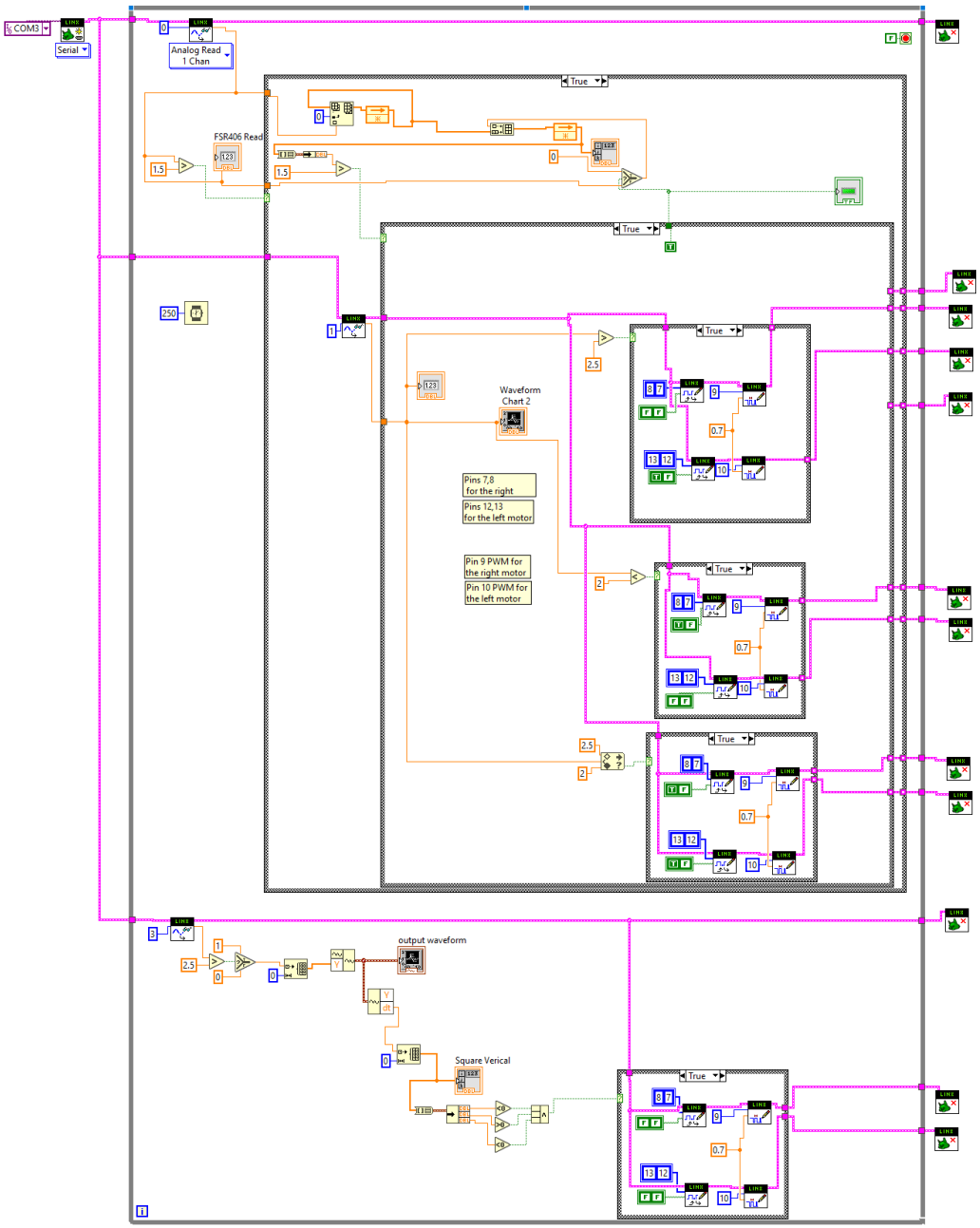

Figure 5.17: Overall Code with All Cases True

Figure 5.18 shows the overall code with cases false.

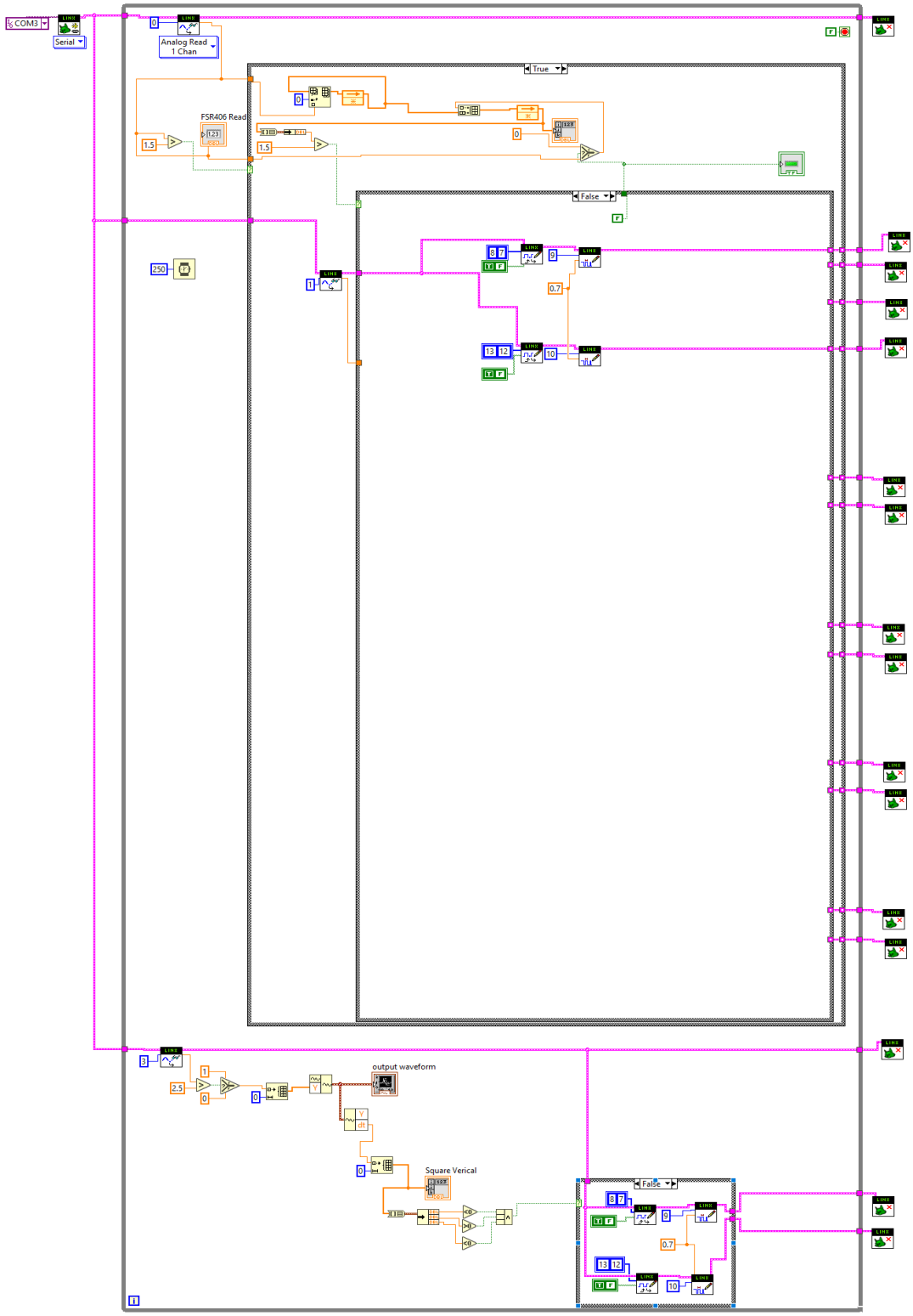

Figure 5.18: Overall Code with Cases False

5.6 NI-myRio-1900 Controller

Using Linx library with labview software decreases the efficiency of the Arduino controller in which it can't give the wanted frequency for the driver, so myRio-1900 controller is used.

The National Instruments myRIO-1900 is a portable reconfigurable I/O (RIO) device that can be used to design control, robotics, and mechatronics systems. Figure 5.19 shows the myRio-1900 controller.

Figure 5.19: NI myRio-1900 Controller

5.6.1 NI myRio-1900 features

NI myRio-1900 has three I/O ports to be connected with digital and analog inputs and outputs; figure 5.20 illustrates the three ports of the controller.

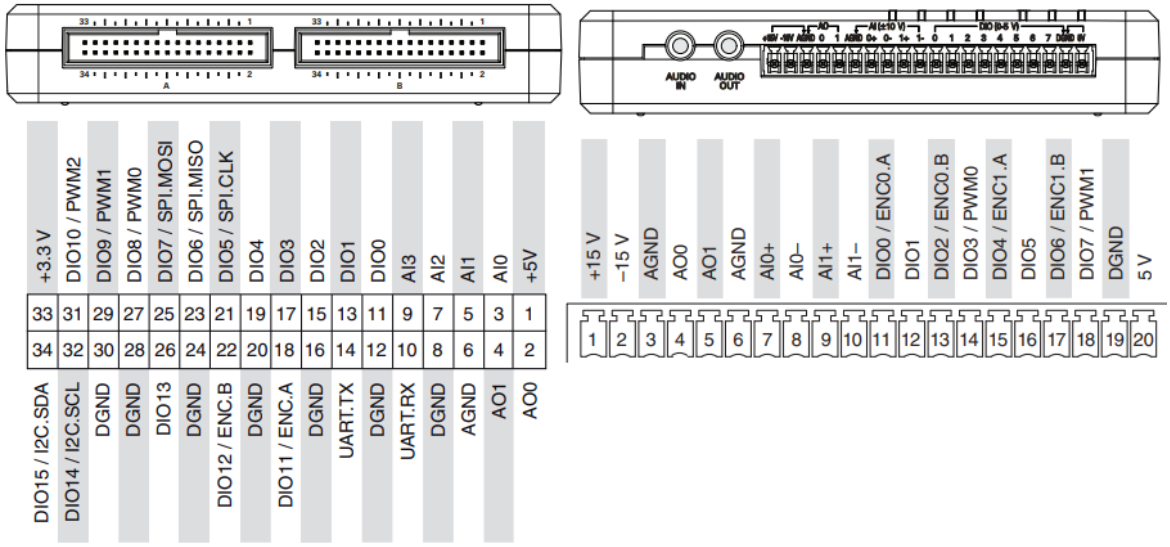

Figure 5.20: Ports A,B and C for myRio-1900 controller

Table 5.4 shows the main features of the myRio-1900 controller, which meets the needs of the driver.

Table 5.4: NImyRio-1900 main features.

Processor speed	667MHz
Analog input resolution	12 bits
Overvoltage protection	±16V
Analog Inputs	6 (for all ports)
Analog Outputs	4 (for all ports)
Digital I/O	22 (for all ports)
PWM	100 kHz
Power supply	6 to 13V DC
Ambient temperature	0-40 C^o

5.6.2 NImyRio Code

Making the code of the myRio controller just needs to replace the Linx functions with myRio configuration functions to select PWM frequency, analog and digital I/O pins, and duty cycle. Figure 5.21 shows the code created using myRio controller in case the eye-controlling-system is activated.

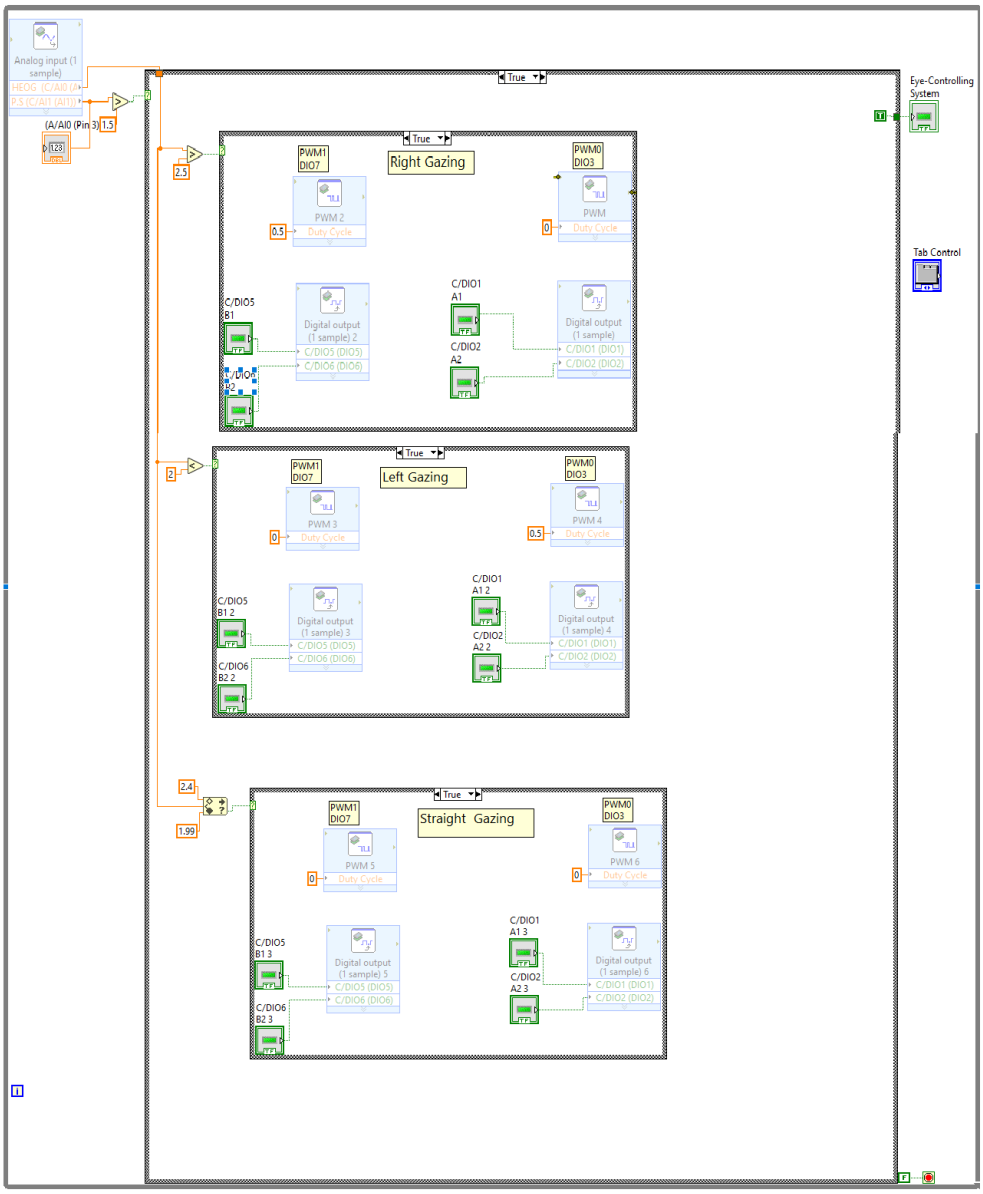

Figure 5.21: Eye-driving-system Code Using myRio in Case True.

Figure 5.22 shows the myRio code in case the eye-driving system is off

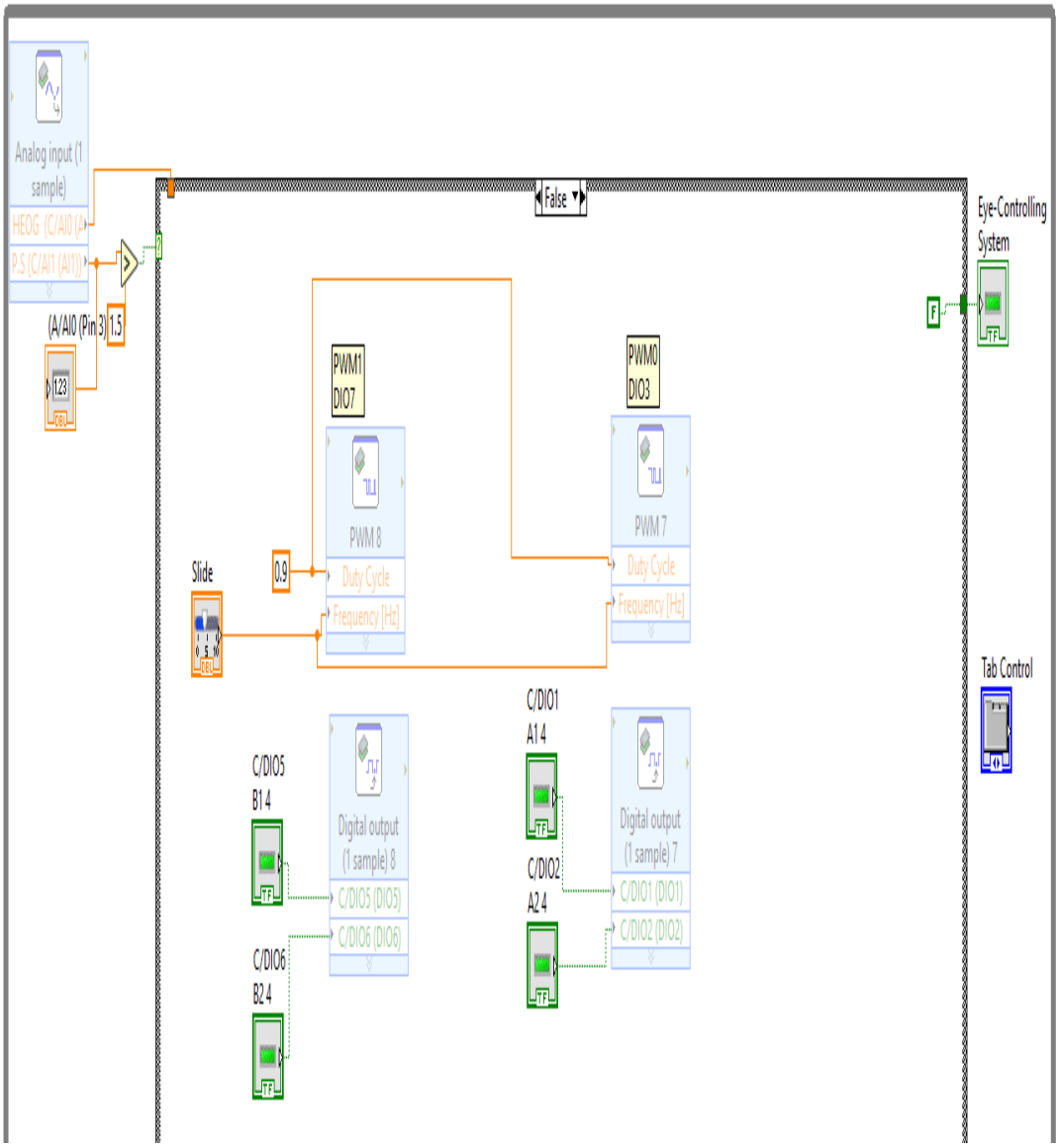

Figure 5.22: Eye-driving-system Code Using myRio in Case False.

5.7 Challenges

Designing an eye-controlling-system is a challenging work, especially in making it to be suitable for people with quadriplegia, the prominent problems in achieving this project:

1- EOG signal is a millivolt signal, which makes it easily affected by any noise, so the filtration step must be very accurate, because of the a fourth order low pass filter is used.

2- The controller which is combatable with LabView software which is myRio is very expensive, its cost starts from 500 dollar, to solve this problem, Linx library is used to upload the LabView code to the Arduino controller.

3- In order to keep the joystick driving system which is built in the wheelchair, a switching system is made between it and the eye-controlling-system driver, the user can switch between driving systems using the switches.

4- To make the usage of the wheelchair safe and comfort for people with quadriplegia, it must be fully controlled by eyes and tongue, so a FlexiForce sensor must be added to the system to control the eye-controlling-system.

5- To prevent any overlapping between right and left gazing EOG values, a safe region is made between 2-2.5 volts, which represents the forward gazing, which makes the wheelchair move forward.

6- The Flexiforce sensor can be used only just for one purpose, so it was just used as a switch for the eye-controlling-system.

7- Vertical eye gazing EOG signal is hard to be analyzed, it is not as simple as horizontal, which made it hard to classify upward gazing.

8- Mounting the FlexiForce sensor on the cheek cause some undesired voltage created by the movement of the cheek, to solve this problem; a threshold of 1.5volt is used as reference, so this value will not be reached unless the user press deliberately on the sensor.

5.8 Using Instructions

Here are the user instructions for using the wheelchair in correct way:

1-Put the electrodes as shown in figure 2.3 in chapter two.

2- Mount the FelxiForce sensor on the cheek in where it is easy to press on it by tongue.

3- Turn OFF the wheelchair switch and turn ON the eye-driving-system switch.

4- Turn ON the wheelchair and EOG switches.

5- To start directing the wheelchair by eyes, press on the FlexiForce sensor and follow table 5.5

6- To stop the eye-driving system press another time on the FelxiForce sensor.

Table 5.5: Wheelchair Control According to Eye Movements

Eye Movement	**Wheelchair control**
Gazing right	Turning right
Gazing left	Turning left
Gazing up	Break

5.9 Future Work

To get the best exploit of the achieved systems, here are some suggestions for a future work:

1- Use the eye-driving-system in modifying cars to be suitable for people with quadriplegia.

2- Implement more accurate coding methods for classification of eye gazing, as more mathematical analysis for the EOG analysis or using artificial intelligence.

3- Get approval for manufacturing this project to be ready for people with quadriplegia's usage.

APPINDIX A

Datasheet for ''AD620A''

ANALOG DEVICES

Low Cost, Low Power Instrumentation Amplifier

AD620

FEATURES
EASY TO USE
Gain Set with One External Resistor
(Gain Range 1 to 1000)
Wide Power Supply Range (±2.3 V to ±18 V)
Higher Performance than Three Op Amp IA Designs
Available in 8-Lead DIP and SOIC Packaging
Low Power, 1.3 mA max Supply Current

EXCELLENT DC PERFORMANCE ("B GRADE")
50 μV max, Input Offset Voltage
0.6 μV/°C max, Input Offset Drift
1.0 nA max, Input Bias Current
100 dB min Common-Mode Rejection Ratio (G = 10)

LOW NOISE
9 nV/√Hz, @ 1 kHz, Input Voltage Noise
0.28 μV p-p Noise (0.1 Hz to 10 Hz)

EXCELLENT AC SPECIFICATIONS
120 kHz Bandwidth (G = 100)
15 μs Settling Time to 0.01%

APPLICATIONS
Weigh Scales
ECG and Medical Instrumentation
Transducer Interface
Data Acquisition Systems
Industrial Process Controls
Battery Powered and Portable Equipment

CONNECTION DIAGRAM

8-Lead Plastic Mini-DIP (N), Cerdip (Q) and SOIC (R) Packages

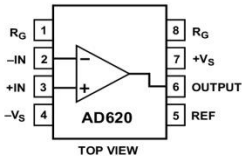

TOP VIEW

PRODUCT DESCRIPTION

The AD620 is a low cost, high accuracy instrumentation amplifier that requires only one external resistor to set gains of 1 to 1000. Furthermore, the AD620 features 8-lead SOIC and DIP packaging that is smaller than discrete designs, and offers lower power (only 1.3 mA max supply current), making it a good fit for battery powered, portable (or remote) applications.

The AD620, with its high accuracy of 40 ppm maximum nonlinearity, low offset voltage of 50 μV max and offset drift of 0.6 μV/°C max, is ideal for use in precision data acquisition systems, such as weigh scales and transducer interfaces. Furthermore, the low noise, low input bias current, and low power of the AD620 make it well suited for medical applications such as ECG and noninvasive blood pressure monitors.

The low input bias current of 1.0 nA max is made possible with the use of Superβeta processing in the input stage. The AD620 works well as a preamplifier due to its low input voltage noise of 9 nV/√Hz at 1 kHz, 0.28 μV p-p in the 0.1 Hz to 10 Hz band, 0.1 pA/√Hz input current noise. Also, the AD620 is well suited for multiplexed applications with its settling time of 15 μs to 0.01% and its cost is low enough to enable designs with one in-amp per channel.

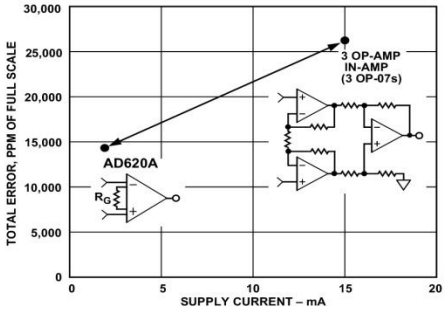

Figure 1. Three Op Amp IA Designs vs. AD620

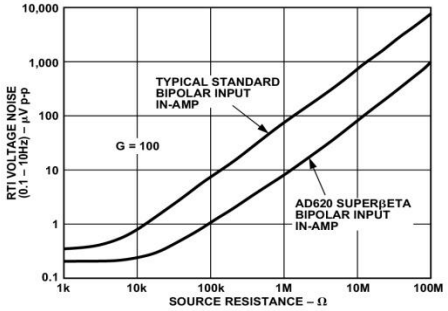

Figure 2. Total Voltage Noise vs. Source Resistance

REV. E

One Technology Way, P.O. Box 9106, Norwood, MA 02062-9106, U.S.A.
Tel: 781/329-4700 World Wide Web Site: http://www.analog.com
Fax: 781/326-8703

AD620—SPECIFICATIONS (Typical @ +25°C, V_S = ±15 V, and R_L = 2 kΩ, unless otherwise noted)

Model	Conditions	AD620A Min	AD620A Typ	AD620A Max	AD620B Min	AD620B Typ	AD620B Max	AD620S[1] Min	AD620S[1] Typ	AD620S[1] Max	Units
GAIN	G = 1 + (49.4 k/R_G)										
Gain Range		1		10,000	1		10,000	1		10,000	
Gain Error[2]	V_{OUT} = ±10 V										
G = 1			0.03	0.10		0.01	0.02		0.03	0.10	%
G = 10			0.15	0.30		0.10	0.15		0.15	0.30	%
G = 100			0.15	0.30		0.10	0.15		0.15	0.30	%
G = 1000			0.40	0.70		0.35	0.50		0.40	0.70	%
Nonlinearity,	V_{OUT} = –10 V to +10 V,										
G = 1–1000	R_L = 10 kΩ		10	40		10	40		10	40	ppm
G = 1–100	R_L = 2 kΩ		10	95		10	95		10	95	ppm
Gain vs. Temperature											
	G =1			10			10			10	ppm/°C
	Gain >1[2]			–50			–50			–50	ppm/°C
VOLTAGE OFFSET	(Total RTI Error = V_{OSI} + V_{OSO}/G)										
Input Offset, V_{OSI}	V_S = ±5 V to ±15 V		30	125		15	50		30	125	µV
Over Temperature	V_S = ±5 V to ±15 V			185			85			225	µV
Average TC	V_S = ±5 V to ±15 V		0.3	1.0		0.1	0.6		0.3	1.0	µV/°C
Output Offset, V_{OSO}	V_S = ±15 V		400	1000		200	500		400	1000	µV
	V_S = ±5 V			1500			750			1500	µV
Over Temperature	V_S = ±5 V to ±15 V			2000			1000			2000	µV
Average TC	V_S = ±5 V to ±15 V		5.0	15		2.5	7.0		5.0	15	µV/°C
Offset Referred to the Input vs. Supply (PSR)	V_S = ±2.3 V to ±18 V										
G = 1		80	100		80	100		80	100		dB
G = 10		95	120		100	120		95	120		dB
G = 100		110	140		120	140		110	140		dB
G = 1000		110	140		120	140		110	140		dB
INPUT CURRENT											
Input Bias Current			0.5	2.0		0.5	1.0		0.5	2	nA
Over Temperature				2.5			1.5			4	nA
Average TC			3.0			3.0			8.0		pA/°C
Input Offset Current			0.3	1.0		0.3	0.5		0.3	1.0	nA
Over Temperature				1.5			0.75			2.0	nA
Average TC			1.5			1.5			8.0		pA/°C
INPUT											
Input Impedance											
Differential			10‖2			10‖2			10‖2		GΩ‖pF
Common-Mode			10‖2			10‖2			10‖2		GΩ‖pF
Input Voltage Range[3]	V_S = ±2.3 V to ±5 V	$–V_S$ + 1.9		$+V_S$ – 1.2	$–V_S$ + 1.9		$+V_S$ – 1.2	$–V_S$ + 1.9		$+V_S$ – 1.2	V
Over Temperature		$–V_S$ + 2.1		$+V_S$ – 1.3	$–V_S$ + 2.1		$+V_S$ – 1.3	$–V_S$ + 2.1		$+V_S$ – 1.3	V
	V_S = ±5 V to ±18 V	$–V_S$ + 1.9		$+V_S$ – 1.4	$–V_S$ + 1.9		$+V_S$ – 1.4	$–V_S$ + 1.9		$+V_S$ – 1.4	V
Over Temperature		$–V_S$ + 2.1		$+V_S$ – 1.4	$–V_S$ + 2.1		$+V_S$ – 1.4	$–V_S$ + 2.3		$+V_S$ – 1.4	V
Common-Mode Rejection Ratio DC to 60 Hz with I kΩ Source Imbalance	V_{CM} = 0 V to ±10 V										
G = 1		73	90		80	90		73	90		dB
G = 10		93	110		100	110		93	110		dB
G = 100		110	130		120	130		110	130		dB
G = 1000		110	130		120	130		110	130		dB
OUTPUT											
Output Swing	R_L = 10 kΩ,										
	V_S = ±2.3 V to ±5 V	$–V_S$ + 1.1		$+V_S$ – 1.2	$–V_S$ + 1.1		$+V_S$ – 1.2	$–V_S$ + 1.1		$+V_S$ – 1.2	V
Over Temperature		$–V_S$ + 1.4		$+V_S$ – 1.3	$–V_S$ + 1.4		$+V_S$ – 1.3	$–V_S$ + 1.6		$+V_S$ – 1.3	V
	V_S = ±5 V to ±18 V	$–V_S$ + 1.2		$+V_S$ – 1.4	$–V_S$ + 1.2		$+V_S$ – 1.4	$–V_S$ + 1.2		$+V_S$ – 1.4	V
Over Temperature		$–V_S$ + 1.6		$+V_S$ – 1.5	$–V_S$ + 1.6		$+V_S$ – 1.5	$–V_S$ + 2.3		$+V_S$ – 1.5	V
Short Current Circuit			±18			±18			±18		mA

Model	Conditions	AD620A Min	AD620A Typ	AD620A Max	AD620B Min	AD620B Typ	AD620B Max	AD620S[1] Min	AD620S[1] Typ	AD620S[1] Max	Units
DYNAMIC RESPONSE											
Small Signal –3 dB Bandwidth											
G = 1			1000			1000			1000		kHz
G = 10			800			800			800		kHz
G = 100			120			120			120		kHz
G = 1000			12			12			12		kHz
Slew Rate		0.75	1.2		0.75	1.2		0.75	1.2		V/μs
Settling Time to 0.01%	10 V Step										
G = 1–100			15			15			15		μs
G = 1000			150			150			150		μs
NOISE											
Voltage Noise, 1 kHz	$Total\ RTI\ Noise = \sqrt{(e^2_{ni}) + (e_{no}/G)^2}$										
Input, Voltage Noise, e_{ni}			9	13		9	13		9	13	nV/√Hz
Output, Voltage Noise, e_{no}			72	100		72	100		72	100	nV/√Hz
RTI, 0.1 Hz to 10 Hz											
G = 1			3.0			3.0	6.0		3.0	6.0	μV p-p
G = 10			0.55			0.55	0.8		0.55	0.8	μV p-p
G = 100–1000			0.28			0.28	0.4		0.28	0.4	μV p-p
Current Noise	f = 1 kHz		100			100			100		fA/√Hz
0.1 Hz to 10 Hz			10			10			10		pA p-p
REFERENCE INPUT											
R_{IN}			20			20			20		kΩ
I_{IN}	V_{IN+}, V_{REF} = 0		+50	+60		+50	+60		+50	+60	μA
Voltage Range		$-V_S + 1.6$		$+V_S - 1.6$	$-V_S + 1.6$		$+V_S - 1.6$	$-V_S + 1.6$		$+V_S - 1.6$	V
Gain to Output			1 ± 0.0001			1 ± 0.0001			1 ± 0.0001		
POWER SUPPLY											
Operating Range[4]		±2.3		±18	±2.3		±18	±2.3		±18	V
Quiescent Current	V_S = ±2.3 V to ±18 V		0.9	1.3		0.9	1.3		0.9	1.3	mA
Over Temperature			1.1	1.6		1.1	1.6		1.1	1.6	mA
TEMPERATURE RANGE											
For Specified Performance		–40 to +85			–40 to +85			–55 to +125			°C

NOTES
[1]See Analog Devices military data sheet for 883B tested specifications.
[2]Does not include effects of external resistor R_G.
[3]One input grounded. G = 1.
[4]This is defined as the same supply range which is used to specify PSR.
Specifications subject to change without notice.

APPINDIX B

Datasheet for ''AD822''

ANALOG DEVICES

Single Supply, Rail-to-Rail Low Power FET-Input Op Amp

AD822

FEATURES
TRUE SINGLE SUPPLY OPERATION
Output Swings Rail to Rail
Input Voltage Range Extends Below Ground
Single Supply Capability from +3 V to +36 V
Dual Supply Capability from ±1.5 V to ±18 V
HIGH LOAD DRIVE
Capacitive Load Drive of 350 pF, G = 1
Minimum Output Current of 15 mA
EXCELLENT AC PERFORMANCE FOR LOW POWER
800 µA Max Quiescent Current per Amplifier
Unity Gain Bandwidth: 1.8 MHz
Slew Rate of 3.0 V/µs
GOOD DC PERFORMANCE
800 µV Max Input Offset Voltage
2 µV/°C Typ Offset Voltage Drift
25 pA Max Input Bias Current
LOW NOISE
13 nV/√Hz @ 10 kHz
NO PHASE INVERSION

APPLICATIONS
Battery Powered Precision Instrumentation
Photodiode Preamps
Active Filters
12- to 14-Bit Data Acquisition Systems
Medical Instrumentation
Low Power References and Regulators

PRODUCT DESCRIPTION

The AD822 is a dual precision, low power FET input op amp that can operate from a single supply of +3.0 V to 36 V, or dual supplies of ±1.5 V to ±18 V. It has true single supply capability with an input voltage range extending below the negative rail, allowing the AD822 to accommodate input signals below ground in the single supply mode. Output voltage swing extends to within 10 mV of each rail providing the maximum output dynamic range.

Offset voltage of 800 µV max, offset voltage drift of 2 µV/°C, input bias currents below 25 pA and low input voltage noise provide dc precision with source impedances up to a Gigaohm. 1.8 MHz unity gain bandwidth, –93 dB THD at 10 kHz and 3 V/µs slew rate are provided with a low supply current of 800 µA per amplifier. The AD822 drives up to 350 pF of direct capacitive load as a follower, and provides a minimum output current of 15 mA. This allows the amplifier to handle a wide range of load conditions. This combination of ac and dc performance, plus the outstanding load drive capability, results in an exceptionally versatile amplifier for the single supply user.

The AD822 is available in four performance grades. The A and B grades are rated over the industrial temperature range of –40°C to +85°C. There is also a 3 volt grade—the AD822A-3V, rated over the industrial temperature range. The mil grade is rated over the military temperature range of –55°C to +125°C and is available processed on standard military drawing.

The AD822 is offered in three varieties of 8-pin package: plastic DIP, hermetic cerdip and surface mount (SOIC) as well as die form.

CONNECTION DIAGRAM
8-Pin Plastic DIP, Cerdip and SOIC

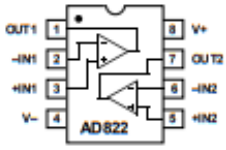

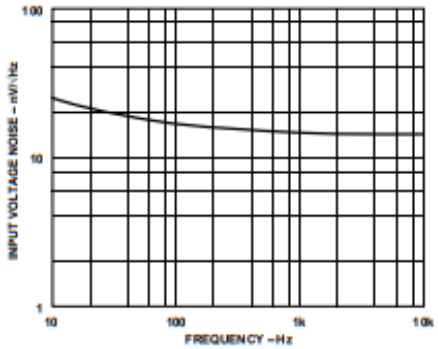

Input Voltage Noise vs. Frequency

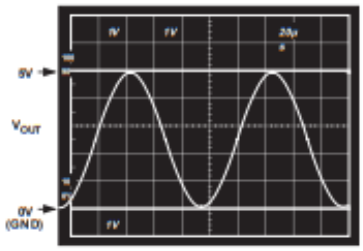

Gain of +2 Amplifier; V_S = +5, 0, V_{IN} = 2.5 V Sine Centered at 1.25 Volts, R_L = 100 kΩ

REV. A

One Technology Way, P.O. Box 9106, Norwood, MA 02062-9106, U.S.A.
Tel: 617/329-4700 Fax: 617/326-8703

AD822–SPECIFICATIONS (V_S = 0, 5 volts @ T_A = +25°C, V_{CM} = 0 V, V_{OUT} = 0.2 V unless otherwise noted)

Parameter	Conditions	AD822A Min	AD822A Typ	AD822A Max	AD822B Min	AD822B Typ	AD822B Max	AD822S[1] Min	AD822S[1] Typ	AD822S[1] Max	Units
DC PERFORMANCE											
Initial Offset			0.1	0.8		0.1	0.4		0.1	0.8	mV
Max Offset over Temperature			0.5	1.2		0.5	0.9		0.5		mV
Offset Drift			2			2			2		µV/°C
Input Bias Current	V_{CM} = 0 V to 4 V		2	25		2	10		2	25	pA
at T_{MAX}			0.5	5		0.5	2.5		0.5		nA
Input Offset Current			2	20		2	10		2	20	pA
at T_{MAX}			0.5			0.5			1.5		nA
Open-Loop Gain	V_O = 0.2 V to 4 V										
	R_L = 100 k	500	1000		500	1000		500	1000		V/mV
T_{MIN} to T_{MAX}		400			400						V/mV
	R_L = 10 k	80	150		80	150		80	150		V/mV
T_{MIN} to T_{MAX}		80			80						V/mV
	R_L = 1 k	15	30		15	30		15	30		V/mV
T_{MIN} to T_{MAX}		10			10						V/mV
NOISE/HARMONIC PERFORMANCE											
Input Voltage Noise											
0.1 Hz to 10 Hz			2			2			2		µV p-p
f = 10 Hz			25			25			25		nV/√Hz
f = 100 Hz			21			21			21		nV/√Hz
f = 1 kHz			16			16			16		nV/√Hz
f = 10 kHz			13			13			13		nV/√Hz
Input Current Noise											
0.1 Hz to 10 Hz			18			18			18		fA p-p
f = 1 kHz			0.8			0.8			0.8		fA/√Hz
Harmonic Distortion	R_L = 10 k to 2.5 V										
f = 10 kHz	V_O = 0.25 V to 4.75 V		–93			–93			–93		dB
DYNAMIC PERFORMANCE											
Unity Gain Frequency			1.8			1.8			1.8		MHz
Full Power Response	V_O p-p = 4.5 V		210			210			210		kHz
Slew Rate			3			3			3		V/µs
Settling Time											
to 0.1%	V_O = 0.2 V to 4.5 V		1.4			1.4			1.4		µs
to 0.01%			1.8			1.8			1.8		µs
MATCHING CHARACTERISTICS											
Initial Offset				1.0			0.5			1.6	mV
Max Offset Over Temperature				1.6			1.3				mV
Offset Drift			3			3					µV/°C
Input Bias Current				20			10			20	pA
Crosstalk @ f = 1 kHz	R_L = 5 kΩ		–130			–130			–130		dB
f = 100 kHz			–93			–93			–93		dB
INPUT CHARACTERISTICS											
Common-Mode Voltage Range[2]		–0.2		4	–0.2		4	–0.2		4	V
T_{MIN} to T_{MAX}		–0.2		4	–0.2		4				V
CMRR	V_{CM} = 0 V to +2 V	66	80		69	80		66	80		dB
T_{MIN} to T_{MAX}		66			66						dB
Input Impedance											
Differential			10^{13}‖0.5			10^{13}‖0.5			10^{13}‖0.5		Ω‖pF
Common Mode			10^{13}‖2.8			10^{13}‖2.8			10^{13}‖2.8		Ω‖pF
OUTPUT CHARACTERISTICS											
Output Saturation Voltage[3]											
V_{OL}–V_{EE}	I_{SINK} = 20 µA		5	7		5	7		5	7	mV
T_{MIN} to T_{MAX}				10			10				mV
V_{CC}–V_{OH}	I_{SOURCE} = 20 µA		10	14		10	14		10	14	mV
T_{MIN} to T_{MAX}				20			20				mV
V_{OL}–V_{EE}	I_{SINK} = 2 mA		40	55		40	55		40	55	mV
T_{MIN} to T_{MAX}				80			80				mV
V_{CC}–V_{OH}	I_{SOURCE} = 2 mA		80	110		80	110		80	110	mV
T_{MIN} to T_{MAX}				160			160				mV
V_{OL}–V_{EE}	I_{SINK} = 15 mA		300	500		300	500		300	500	mV
T_{MIN} to T_{MAX}				1000			1000				mV
V_{CC}–V_{OH}	I_{SOURCE} = 15 mA		800	1500		800	1500		800	1500	mV
T_{MIN} to T_{MAX}				1900			1900				mV
Operating Output Current		15			15			15			mA
T_{MIN} to T_{MAX}		12			12						mA
Capacitive Load Drive			350			350			350		pF
POWER SUPPLY											
Quiescent Current T_{MIN} to T_{MAX}			1.24	1.6		1.24	1.6		1.24		mA
Power Supply Rejection	V_S+ = 5 V to 15 V	70	80		66	80		70	80		dB
T_{MIN} to T_{MAX}		70			66						dB

AD822–SPECIFICATIONS (V_S = ±15 volts @ T_A = +25°C, V_{CM} = 0 V, V_{OUT} = 0 V unless otherwise noted)

Parameter	Conditions	AD822A			AD822B			AD822S[1]			Units
		Min	Typ	Max	Min	Typ	Max	Min	Typ	Max	
DC PERFORMANCE											
Initial Offset			0.4	2		0.3	1.5		0.4	2.0	mV
Max Offset over Temperature			0.5	3		0.5	2.5		0.5		mV
Offset Drift			2			2			2		µV/°C
Input Bias Current	V_{CM} = 0 V		2	25		2	12		2	25	pA
	V_{CM} = –10 V		40			40			40		pA
at T_{MAX}	V_{CM} = 0 V		0.5	5		0.5	2.5		0.5		nA
Input Offset Current			2	20		2	12		2	20	pA
at T_{MAX}			0.5			0.5			1.5		nA
Open-Loop Gain	V_O = +10 V to –10 V										
	R_L = 100 k	500	2000		500	2000		500	2000		V/mV
T_{MIN} to T_{MAX}		500			500						V/mV
	R_L = 10 k	100	500		100	500		150	400		V/mV
T_{MIN} to T_{MAX}		100			100						V/mV
	R_L = 1 k	30	45		30	45		30	45		V/mV
T_{MIN} to T_{MAX}		20			20						V/mV
NOISE/HARMONIC PERFORMANCE											
Input Voltage Noise											
0.1 Hz to 10 Hz			2			2			2		µV p-p
f = 10 Hz			25			25			25		nV/√Hz
f = 100 Hz			21			21			21		nV/√Hz
f = 1 kHz			16			16			16		nV/√Hz
f = 10 kHz			13			13			13		nV/√Hz
Input Current Noise											
0.1 Hz to 10 Hz			18			18			18		fA p-p
f = 1 kHz			0.8			0.8			0.8		fA/√Hz
Harmonic Distortion	R_L = 10 k										
f = 10 kHz	V_O = ±10 V		–85			–85			–85		dB
DYNAMIC PERFORMANCE											
Unity Gain Frequency			1.9			1.9			1.9		MHz
Full Power Response	V_O p-p = 20 V		45			45			45		kHz
Slew Rate			3			3			3		V/µs
Settling Time											
to 0.1%	V_O = 0 V to ±10 V		4.1			4.1			4.1		µs
to 0.01%			4.5			4.5			4.5		µs
MATCHING CHARACTERISTICS											
Initial Offset				3			2			0.8	mV
Max Offset Over Temperature				4			2.5			1.0	mV
Offset Drift			3			3					µV/°C
Input Bias Current				25			12			25	pA
Crosstalk @ f = 1 kHz	R_L = 5 kΩ		–130			–130			–130		dB
f = 100 kHz			–93			–93			–93		dB
INPUT CHARACTERISTICS											
Common-Mode Voltage Range[2]		–15.2		14	–15.2		14	–15.2		14	V
T_{MIN} to T_{MAX}		–15.2		14	–15.2		14				V
CMRR	V_{CM} = –15 V to 12 V	70	80		74	90		70	90		dB
T_{MIN} to T_{MAX}		70			74						dB
Input Impedance											
Differential			10^{13}‖0.5			10^{13}‖0.5			10^{13}‖0.5		Ω‖pF
Common Mode			10^{13}‖2.8			10^{13}‖2.8			10^{13}‖2.8		Ω‖pF
OUTPUT CHARACTERISTICS											
Output Saturation Voltage[3]											
V_{OL}–V_{EE}	I_{SINK} = 20 µA		5	7		5	7		5	7	mV
T_{MIN} to T_{MAX}				10			10				mV
V_{CC}–V_{OH}	I_{SOURCE} = 20 µA		10	14		10	14		10	14	mV
T_{MIN} to T_{MAX}				20			20				mV
V_{OL}–V_{EE}	I_{SINK} = 2 mA		40	55		40	55		40	55	mV
T_{MIN} to T_{MAX}				80			80				mV
V_{CC}–V_{OH}	I_{SOURCE} = 2 mA		80	110		80	110		80	110	mV
T_{MIN} to T_{MAX}				160			160				mV
V_{OL}–V_{EE}	I_{SINK} = 15 mA		300	500		300	500		300	500	mV
T_{MIN} to T_{MAX}				1000			1000				mV
V_{CC}–V_{OH}	I_{SOURCE} = 15 mA		800	1500		800	1500		800	1500	mV
T_{MIN} to T_{MAX}				1900			1900				mV
Operating Output Current		20			20			20			mA
T_{MIN} to T_{MAX}		15			15						mA
Capacitive Load Drive			350			350			350		pF
POWER SUPPLY											
Quiescent Current T_{MIN} to T_{MAX}			1.4	1.8		1.4	1.8		1.4		mA
Power Supply Rejection	V_S+ = 5 V to 15 V	70	80		70	80		70	80		dB
T_{MIN} to T_{MAX}		70			70						dB

(V_S = 0, 3 volts @ T_A = +25°C, V_{CM} = 0 V, V_{OUT} = 0.2 V unless otherwise noted)

Parameter	Conditions	AD822A-3 V Min	Typ	Max	Units
DC PERFORMANCE					
Initial Offset			0.2	1	mV
Max Offset over Temperature			0.5	1.5	mV
Offset Drift			1		µV/°C
Input Bias Current	V_{CM} = 0 V to +2 V		2	25	pA
at T_{MAX}			0.5	5	nA
Input Offset Current			2	20	pA
at T_{MAX}			0.5		nA
Open-Loop Gain	V_O = 0.2 V to 2 V				
	R_L = 100 k	300	1000		V/mV
T_{MIN} to T_{MAX}		300			V/mV
	R_L = 10 k	60	150		V/mV
T_{MIN} to T_{MAX}		60			V/mV
	R_L = 1 k	10	30		V/mV
T_{MIN} to T_{MAX}		8			V/mV
NOISE/HARMONIC PERFORMANCE					
Input Voltage Noise					
0.1 Hz to 10 Hz			2		µV p-p
f = 10 Hz			25		nV/√Hz
f = 100 Hz			21		nV/√Hz
f = 1 kHz			16		nV/√Hz
f = 10 kHz			13		nV/√Hz
Input Current Noise					
0.1 Hz to 10 Hz			18		fA p-p
f = 1 kHz			0.8		fA/√Hz
Harmonic Distortion	R_L = 10 k to 1.5 V				
f = 10 kHz	V_O = ±1.25 V		–92		dB
DYNAMIC PERFORMANCE					
Unity Gain Frequency			1.5		MHz
Full Power Response	V_O p-p = 2.5 V		240		kHz
Slew Rate			3		V/µs
Settling Time					
to 0.1%	V_O = 0.2 V to 2.5 V		1		µs
to 0.01%			1.4		µs
MATCHING CHARACTERISTICS					
Initial Offset				1	mV
Max Offset Over Temperature				2	mV
Offset Drift			2		µV/°C
Input Bias Current				10	pA
Crosstalk @ f = 1 kHz	R_L = 5 kΩ		–130		dB
f = 100 kHz			–93		dB
INPUT CHARACTERISTICS					
Common-Mode Voltage Range[2]		–0.2		2	V
T_{MIN} to T_{MAX}		–0.2		2	V
CMRR	V_{CM} = 0 V to +1 V	60	74		dB
T_{MIN} to T_{MAX}		60			dB
Input Impedance					
Differential			10^{13}‖0.5		Ω‖pF
Common Mode			10^{13}‖2.8		Ω‖pF
OUTPUT CHARACTERISTICS					
Output Saturation Voltage[3]					
V_{OL}–V_{EE}	I_{SINK} = 20 µA		5	7	mV
T_{MIN} to T_{MAX}				10	mV
V_{CC}–V_{OH}	I_{SOURCE} = 20 µA		10	14	mV
T_{MIN} to T_{MAX}				20	mV
V_{OL}–V_{EE}	I_{SINK} = 2 mA		40	55	mV
T_{MIN} to T_{MAX}				80	mV
V_{CC}–V_{OH}	I_{SOURCE} = 2 mA		80	110	mV
T_{MIN} to T_{MAX}				160	mV
V_{OL}–V_{EE}	I_{SINK} = 10 mA		200	400	mV
T_{MIN} to T_{MAX}				400	mV
V_{CC}–V_{OH}	I_{SOURCE} = 10 mA		500	1000	mV
T_{MIN} to T_{MAX}				1000	mV
Operating Output Current		15			mA
T_{MIN} to T_{MAX}		12			mA
Capacitive Load Drive			350		pF
POWER SUPPLY					
Quiescent Current T_{MIN} to T_{MAX}			1.24	1.6	mA
Power Supply Rejection	V_S+ = 3 V to 15 V	70	80		dB
T_{MIN} to T_{MAX}		70			dB

APPINDIX C

Arduino 3 mod B+ pin specification

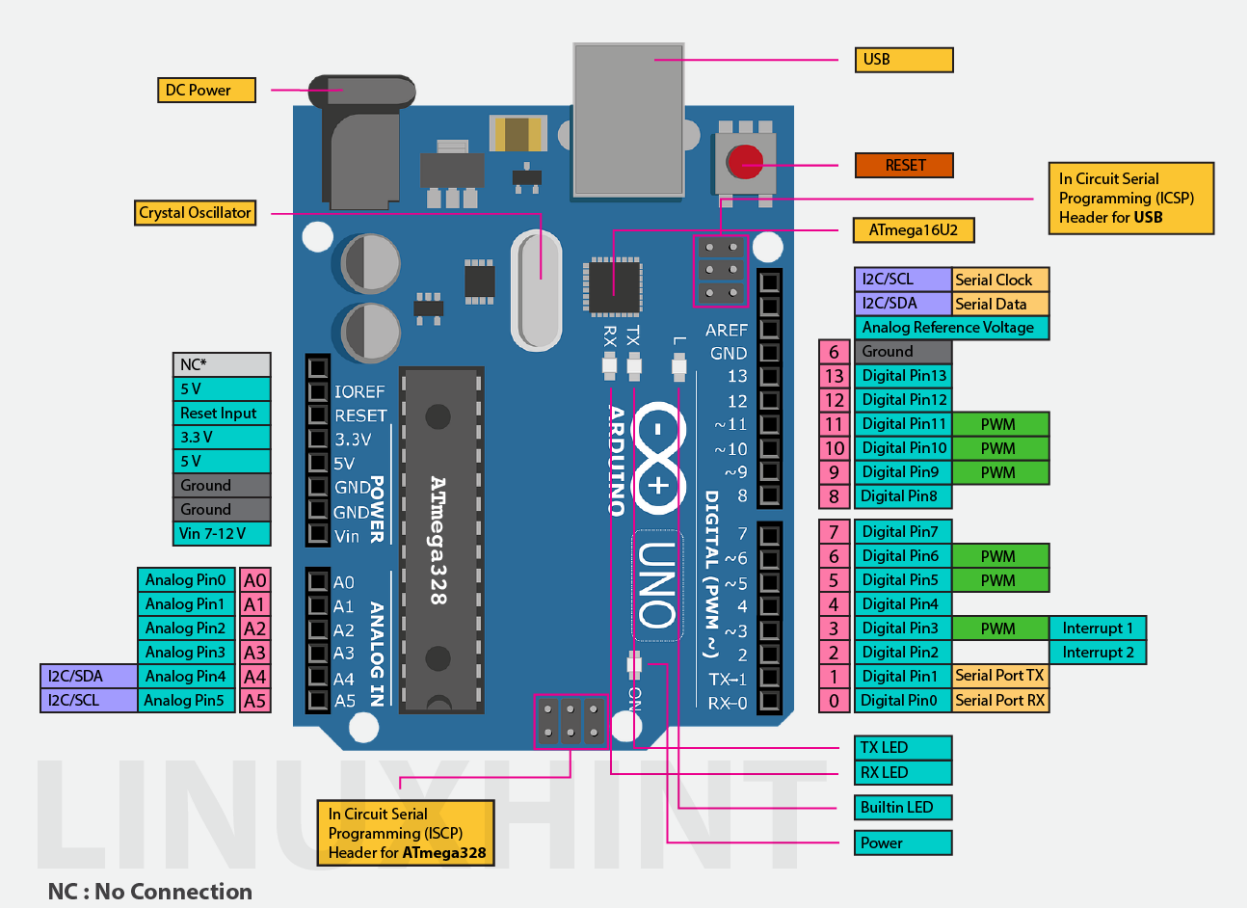

APPINDIX D

FSR406 Pressure Sensor

INTERLINK ELECTRONICS
Sensor Technologies

FSR 406 Data Sheet

FSR 400 Series Square Force Sensing Resistor

Features and Benefits

- Actuation Force as low as 0.1N and sensitivity range to 10N.
- Easily customizable to a wide range of sizes
- Highly Repeatable Force Reading; As low as 2% of initial reading with repeatable actuation system
- Cost effective
- Ultra thin; 0.45mm
- Robust; up to 10M actuations
- Simple and easy to integrate

Industry Segments

- Game controllers
- Musical instruments
- Medical device controls
- Remote controls
- Navigation Electronics
- Industrial HMI
- Automotive Panels
- Consumer Electronics

Description

Interlink Electronics FSR™ 400 series is part of the single zone Force Sensing Resistor™ family. Force Sensing Resistors, or FSRs, are robust polymer thick film (PTF) devices that exhibit a decrease in resistance with increase in force applied to the surface of the sensor. This force sensitivity is optimized for use in human touch control of electronic devices such as automotive electronics, medical systems, and in industrial and robotics applications.

The standard 406 sensor is a square sensor 43.69mm in size. Custom sensors can be manufactured in sizes ranging from 5mm to over 600mm.

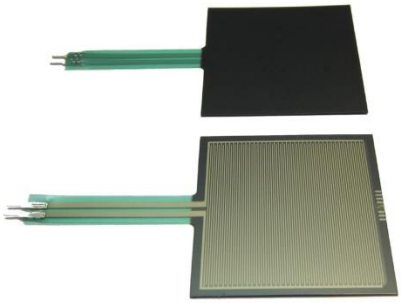

Figure 1 - Typical Force Curve

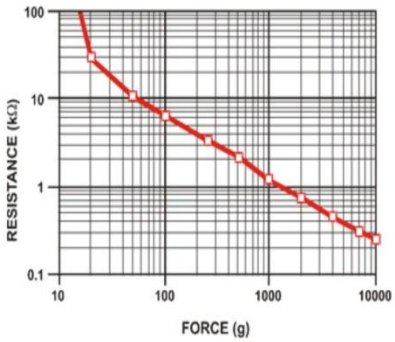

Figure 2 - Typical Schematic

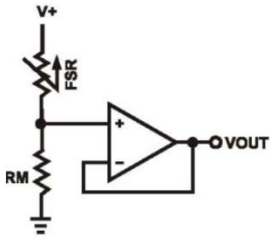

Interlink Electronics - Sensor Technologies

www.interlinkelectronics.com

INTERLINK ELECTRONICS
Sensor Technologies

FSR 406
P/N: 30-73258

Applications

Detect & qualify press
Sense whether a touch is accidental or intended by reading force

Use force for UI feedback
Detect more or less user force to make a more intuitive interface

Enhance tool safety
Differentiate a grip from a touch as a safety lock

Find centroid of force
Use multiple sensors to determine centroid of force

Detect presence, position, or motion
Of a person or patient in a bed, chair, or medical device

Detect liquid blockage
Detect tube or pump occlusion or blockage by measuring back pressure

Detect tube positioning

Many other force measurement applications

Device Characteristics

Feature	Condition	Value*	Notes
Actuation Force		0.1 Newtons	
Force Sensitivity Range		0.1 - 10.0[2] Newtons	
Force Repeatability[3]	(Single part)	± 2%	
Force Resolution[3]		continuous	
Force Repeatability[3]	(Part to Part)	±6%	
Non-Actuated Resistance		10M W	
Size		43.69 x 43.69mm	
Thickness Range		0.2 - 1.25 mm	
Stand-Off Resistance		>10M ohms	Unloaded, unbent
Switch Travel	(Typical)	0.05 mm	Depends on design
Hysteresis[3]		+10%	$(R_{F+} - R_{F-})/R_{F+}$
Device Rise Time		<3 microseconds	measured w/steel ball
Long Term Drift		<5% per $\log_{10}$(time)	35 days test, 1kg load
Temp Operating Range	(Recommended)	-30 - +70 °C	
Number of Actuations	(Life time)	10 Million tested	Without failure

* Specifications are derived from measurements taken at 1000 grams, and are given as one standard deviation / mean, unless otherwise noted.

1. Max Actuation force can be modified in custom sensors.
2. Force Range can be increased in custom sensors. Interlink Electronics have designed and manufactured sensors with operating force larger than 50Kg.
3. Force sensitivity dependent on mechanics, and resolution depends on measurement electronics.

APPINDIX E

"DC motor driver "

ARDUINO

60A High Power MOS Dual Channel H-bridge DC Motor Driver Module

Description:

This module is super wide voltage motor drive (theory highest can amount to 60V), general can achieve 48v, using high quality power MOS, Therefore, the max. Current can be up to 60A. This module can be used for general high power DC motor drive, stable performance, therefore, very suitable for robot competition, a chariot race, Freescale competition, etc.

Features:

1- Use SMT, high integration, superior layout design, very beautiful, small size, built-in 2 channel high power DC motor drive, drive module size only 70mm * 56 mm.
2- Wide heat sink in the large current may be effective for drive module heat, keep good stable Performance.
3- The module maximum rated current 60A, and the on resistance only 0.003 ohms.
4- Switch frequency is high, the most accessible 60KHZ, so effective to debug motor.
5- Control interface is very simple: A1, A2 = 0.0 for brake; A1, A2 = 1.0 for forward; A1, A2 = 0.1 for Reverse.PA for PWM wave input (motor speed regulation): G for common Ground (B channel for the same control).
6- All MCU of 3.3 V and 5 V are can control this module, and only need one channel motor power supply (12 V ~ 48V).

Specifications:

1) Size: 70 mm * 56 mm * 18 mm
2) Positioning Hole :Diameter=3 mm ,4 holes distribution, the spacing for 62 mm * 48 mm.

More Detailed Photos:

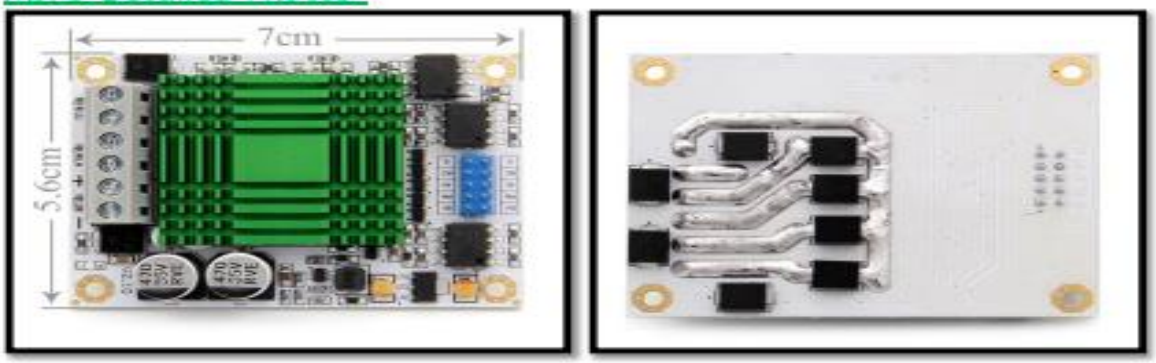

Made in China

APPINDIX F

" NI myRIO-1900"

USER GUIDE AND SPECIFICATIONS

NI myRIO-1900

The National Instruments myRIO-1900 is a portable reconfigurable I/O (RIO) device that students can use to design control, robotics, and mechatronics systems. This document contains pinouts, connectivity information, dimensions, mounting instructions, and specifications for the NI myRIO-1900.

Figure 1. NI myRIO-1900

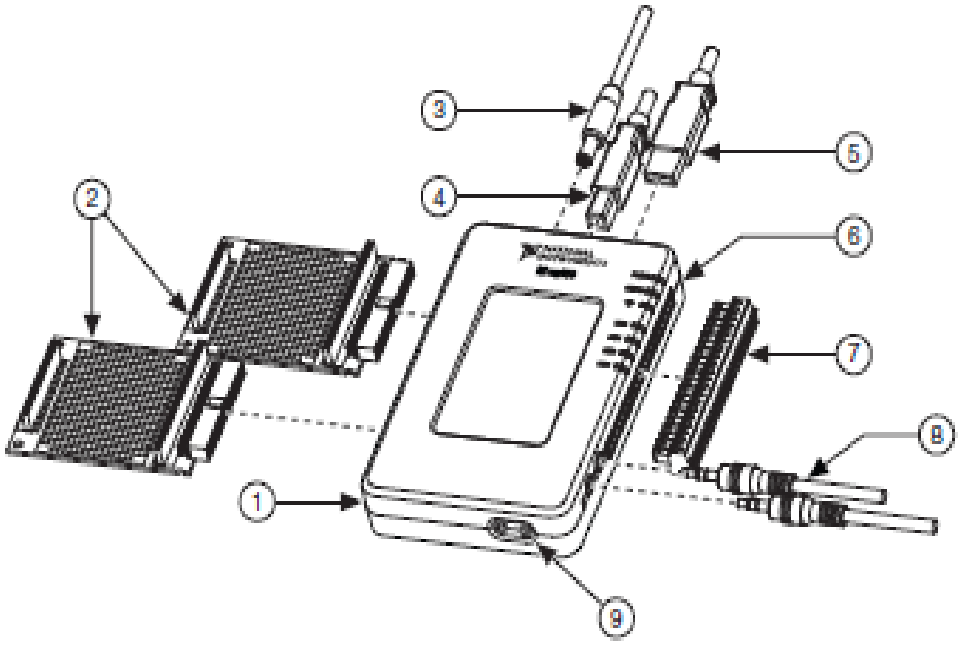

1	NI myRIO-1900	6	LEDs
2	myRIO Expansion Port (MXP) Breakouts (One Included In Kit)	7	Mini System Port (MSP) Screw-Terminal Connector
3	Power Input Cable	8	Audio In/Out Cables (One Included In Kit)
4	USB Device Cable	9	Button0
5	USB Host Cable (Not Included In Kit)		

Hardware Overview

The NI myRIO-1900 provides analog input (AI), analog output (AO), digital input and output (DIO), audio, and power output in a compact embedded device. The NI myRIO-1900 connects to a host computer over USB and wireless 802.11b,g,n.

The following figure shows the arrangement and functions of NI myRIO-1900 components.

Figure 2. NI myRIO-1900 Hardware Block Diagram

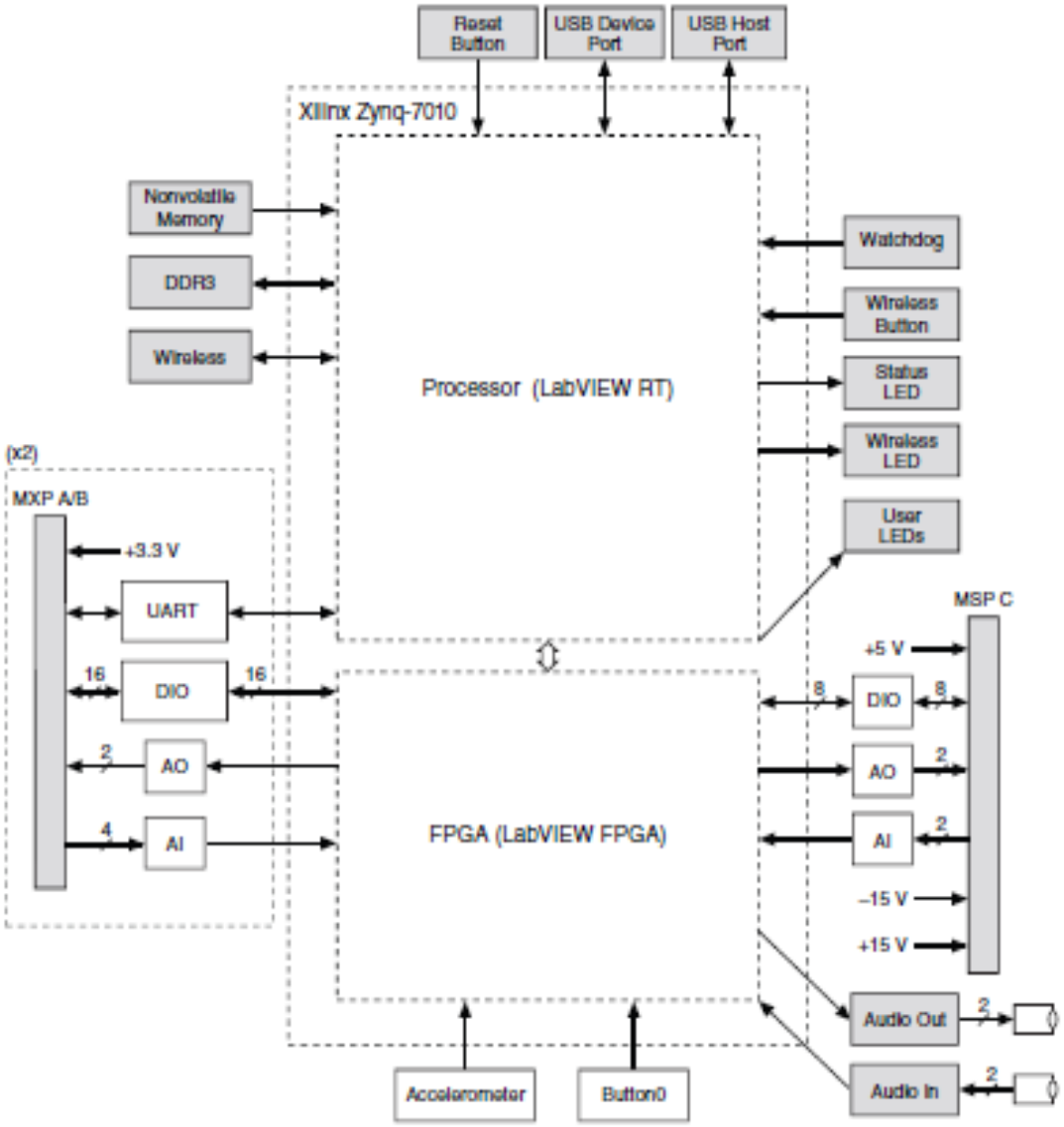

The following figure and table show the signals on Mini System Port (MSP) connector C. Note that some pins carry secondary functions as well as primary functions.

Figure 4. Primary/Secondary Signals on MSP Connector C

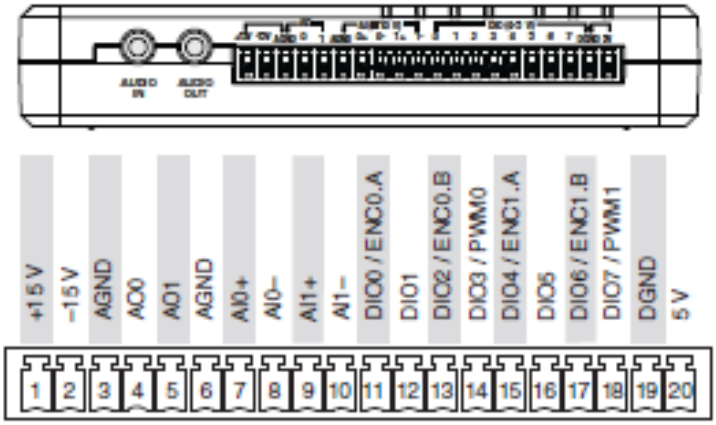

Table 2. Descriptions of Signals on MSP Connector C

Signal Name	Reference	Direction	Description
+15V/-15V	AGND	Output	+15 V/-15 V power output.
AI0+/AI0-; AI1+/AI1-	AGND	Input	±10 V, differential analog input channels. Refer to the *Analog Input Channels* section for more information.
AO <0..1>	AGND	Output	±10 V referenced, single-ended analog output channels. Refer to the *Analog Output Channels* section for more information.
AGND	N/A	N/A	Reference for analog input and output and +15 V/-15 V power output.
+5V	DGND	Output	+5 V power output.
DIO <0..7>	DGND	Input or Output	General-purpose digital lines with 3.3 V output, 3.3 V/5 V-compatible input. Refer to the *DIO Lines* section for more information.
DGND	N/A	N/A	Reference for digital lines and +5 V power output.

Table 3. Descriptions of Signals on Audio Connectors

Signal Name	Reference	Direction	Description
AUDIO IN	N/A	Input	Left and right audio inputs on stereo connector.
AUDIO OUT	N/A	Output	Left and right audio outputs on stereo connector.

Analog Input Channels

The NI myRIO-1900 has analog input channels on myRIO Expansion Port (MXP) connectors A and B, Mini System Port (MSP) connector C, and a stereo audio input connector. The analog inputs are multiplexed to a single analog-to-digital converter (ADC) that samples all channels.

MXP connectors A and B have four single-ended analog input channels per connector, AI0-AI3, which you can use to measure 0-5 V signals. MSP connector C has two high-impedance, differential analog input channels, AI0 and AI1, which you can use to measure signals up to ±10 V. The audio inputs are left and right stereo line-level inputs with a ±2.5 V full-scale range.

Note For important information about improving measurement accuracy by reducing noise, go to `ni.com/info` and enter the Info Code `analogwiring`.

Figure 5 shows the analog input topology of the NI myRIO-1900.

Figure 5. NI myRIO-1900 Analog Input Circuitry

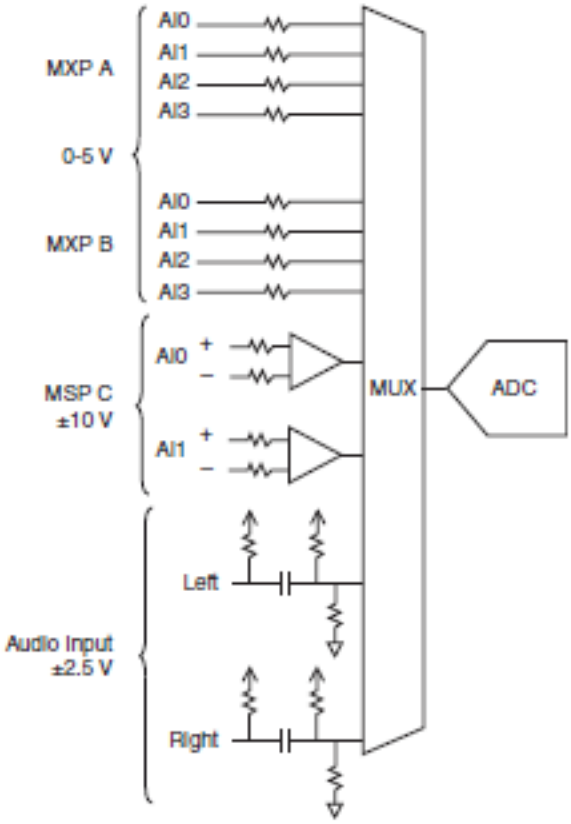

Analog Output Channels

The NI myRIO-1900 has analog output channels on myRIO Expansion Port (MXP) connectors A and B, Mini System Port (MSP) connector C, and a stereo audio output connector. Each analog output channel has a dedicated digital-to-analog converter (DAC), so they can all update simultaneously. The DACs for the analog output channels are controlled by two serial communication buses from the FPGA. MXP connectors A and B share one bus, and MSP connector C and the audio outputs share a second bus. Therefore, the maximum update rate is specified as an aggregate figure in the *Analog Output* section of the *Specifications*.

MXP connectors A and B have two analog output channels per connector, AO0 and AO1, which you can use to generate 0-5 V signals. MSP connector C has two analog output channels, AO0 and AO1, which you can use to generate signals up to ±10 V. The audio outputs are left and right stereo line-level outputs capable of driving headphones.

References1:

1- https://arxiv.org/ftp/arxiv/papers/1312/1312.6410.pdf

2- https://info.wafa.ps/ar_page.aspx?id=8209

3- https://www.alaraby.co.uk/politics/%D8%A5%D8%B5%D8%A7%D8%A8%D8%A9-%D9%81%D9%84%D8%B3%D8%B7%D9%8A%D9%86%D9%8A-%D8%A8%D8%B4%D9%84%D9%84-%D8%B1%D8%A8%D8%A7%D8%B9%D9%8A-%D8%AC%D8%B1%D8%A7%D8%A1-%D8%B1%D8%B5%D8%A7%D8%B5%D8%A9-%D8%A5%D8%B3%D8%B1%D8%A7%D8%A6%D9%8A%D9%84%D9%8A%D8%A9-%D9%85%D9%86-%D9%85%D8%B3%D8%A7%D9%81%D8%A9-%D8%A7%D9%84%D8%B5%D9%81%D8%B1

4- https://www.pcbs.gov.ps/Downloads/book2545.pdf

5- https://www.spinalcord.com/quadriplegia-tetraplegia

References2:

1- OKAMOTO, Takeo, et al. "Using gaze point estimation and blink detection, to control robot arm by use of the EOG signal." Journal of the Japan Society of Applied Electromagnetics and Mechanics 22.2 (2014): 312-317.

2- https://www.spine-health.com/glossary/quadriplegia

3- https://www.spinalcord.com/

References 3

References

1- Roy Choudhury S, Venkataramanan S., Harshal B. Nemade, Sahambi J.S., “Design and Development of a Novel EOG Biopotential Amplifier”, IJBEM Vol. 7, No.1, 2005.

2- Subash Khanal, Rajesh N., Prajwal Bhandari, Design of EOG based HumanMachine Interface system, 4 (2016), pp8.

3- Anwesha Banerjeea, Shreyasi Dattab, Monalisa Palb, Amit Konarb, D.N. Tibarewalaa and R. Janarthanan, Classifying Electrooculogram to Detect DirectionalEye Movements, Data Acquisition System, 10 (2013).

4- Ulrich Sommer J, Birk R, Hörmann K, Stuck BA. Evaluation of the maximumisometric tongue force of healthy volunteers. Eur Arch Otorhinolaryngol. 2014 Nov;271(11):3077-84. doi: 10.1007/s00405-014-3103-6. Epub 2014 Jun 27.

5- Ditte Svane-Knudsen, The tongue is the future for disabled people, 4 (2012), Available at https://sciencenordic.com/denmark-disability-diseases/the-tongue-is- the-future-for-disabled-people/1372887, (last visit 2/11/2021)

6- ElectanTeam, FLEXIFORCE PRESSURE SENSOR, 2(2019), Available at https://www.electan.com/flexiforce-pressure-sensor-25lbs-p-4360-en.html. (Last visit: 21/12/2021.)

7- Made In China, Xex761D Sensor, (2020), Available at https://m.made-in- china.com/product/Xex761d-Miniature-Pressure-Sensor-High-Precision-Small- Space-Force-Measurement-Small-Force-Sensor-Weighing-887294705.html. (Last visit: 21/12/2021)

8- InterlinkTeam, FSR406, (2019), Available at https://www.interlinkelectronics.com/fsr-406. (Last visit: 21/12/2021)

9 - Electrical4U, Electric Motor: What is it? (Types of Electrical Motors), 6(2021),Available at https://www.electrical4u.com/electrical-motor-types-classification-and-history-of-motor/.(last visit 2/11/2021)

10 - Radionics, The Complete Guide to DC Motors, 1(2021), pp4, Available at https://ie.rs-online.com/web/generalDisplay.html?id=ideas-and-advice/dc-motors-guide, (last visit 3/11/2021).

11 - Electrical4U, Brushless DC Motors (BLDC): What Are They & How Do TheyWork?, pp 3, 1(2020), Available at https://www.electrical4u.com/brushless-dc- motors/.

References 4

1- Purnima Singh, Cutoff Frequency Calculator, 4(2021), Available at https://www.omnicalculator.com/physics/cutoff-frequency#:~:text=We%20can%20write%20the%20cutoff,%CF%80%20*%20R%20*%20C%20)%20.&text=fc%20%3D%20636.6%20Hz%20, last visit 15/12/2021.

2- Muhammad Zahak Jamal, Signal Acquisition Using Surface EMG and Circuit DesignConsiderations for Robotic Prosthesis, 4(2012), PP 24.

3- Saed Olfat, Interfacing L298N DC Motor Driver Module with Arduino, 2(2019), Available at https://electropeak.com/learn/interfacing-l298n-motor-driver-controller-module-with-arduino, Lastvisit 15/12/2021